

## ABSTRACT

Title of Document:                    BLOOD    COAGULATION    INDUCING  
   SYNTHETIC POLYMER HYDROGEL

Brendan John Casey, Doctor of Philosophy,  
2010

Directed By:                            Professor Peter Kofinas, Fischell Department of  
   Bioengineering

Uncontrolled hemorrhaging, or blood loss, accounts for upwards of 3 million deaths each year and is the leading cause of preventable deaths after hospital admission around the world. Biological-based hemostatics are quite effective at controlling blood loss, but prohibitively expensive for people in developing countries where over 90 % of these deaths are occurring. Synthetic-based hemostatics are less expensive, yet not nearly as effective as their biological counterparts. A better understanding of how synthetic materials interact with and affect the body's natural clotting response is vital to the development of future hemostatic material technology which will help millions around the world.

Initial in vitro experimentation focused on investigating the key chemical and structural material properties which affect Factor VII (FVII) activation in citrated human plasma. Enzyme-linked assays were utilized to confirm the ability of

specifically formulated charged hydrogels to induce FVII activation and provided insight into the critical material parameters involved in this activation. Dynamic mechanical analysis was used to establish a correlation between polymeric microstructure and FVII activation. Experiments utilizing coagulation factor depleted and inhibited plasmas indicated that FVII, FX, FII, and FI are all vital to the process outlining the general mechanism of fibrin formation from the onset of FVII activation. The ability of the polymer to induce fibrin formation in “artificial plasma” explicitly lacking calcium, TF, and platelets suggested that a specifically designed material surface has the capability to substitute for these vital cofactors.

Clinical diagnostic experimentation using sheep blood indicated that hydrogels containing higher amounts of electrostatic positive charge and lower cross-link density were able to induce faster, more robust clot formation in the presence of a coagulation cascade activator. Subsequent in vivo animal experimentation clearly demonstrated the ability of such hydrogels to aggregate platelets and erythrocytes promoting the formation of an effective hemostatic seal at the wound site. Moreover, in vivo testing confirmed the viability of such a charged polymer hydrogel to effectively control blood loss in a clinically relevant model.

BLOOD COAGULATION INDUCING SYNTHETIC POLYMER HYDROGEL

By

Brendan John Casey

Dissertation submitted to the Faculty of the Graduate School of the  
University of Maryland, College Park, in partial fulfillment  
of the requirements for the degree of  
Doctor of Philosophy  
2010

Advisory Committee:  
Professor Peter Kofinas, Chair/Advisor  
Professor Robert M. Briber  
Professor John P. Fisher  
Professor Sameer B. Shah  
Professor William E. Bentley

© Copyright by  
Brendan John Casey  
2010

## **Dedication**

I would like to dedicate this work to my parents William and Joan Casey who always believed in me and have sacrificed so much for me to get to where I am today.

Thank you.

## **Acknowledgements**

First and foremost I would like to thank my parents Joan and William Casey for all their support throughout my life. I would not be where I am today without their unconditional love and support. I would also like to thank my brother Ryan for always looking out for me, no matter what the situation.

Next I would like to thank my advisor, Professor Peter Kofinas for everything he has done for me over the past 5 years. He is the best teacher I have ever known and I am truly lucky to have found myself under his direction during my graduate career.

Next, I would like to thank Adam Behrens for putting up with me for the past 3 years. He was the best research assistant I could have hoped for and I really appreciate all the hard work he put towards this project over the years. I wish him the best of luck, but at the same time I am confident he will find nothing but success in his future endeavors.

I would also like to say thank you to Dr. Walter Kelley, Dr. John Hess, Dr. Zhongjun Wu, and Dr. Bartley Griffith for all their help with my clinical diagnostic and animal testing. I really appreciate them taking the time out of their busy schedules to assist me with my research. I learned so much from them.

Next, I would like to thank Dr. Robert Briber and the rest of his group members for all their help and incredible insight into my research. I would also like to thank my other committee members Dr. Sameer Shah, Dr. John Fisher, and Dr. William Bentley. They always kept an open door for me throughout the years, and I really appreciate it.

I would also like to thank the A.R.C.S. foundation for their unconditional support throughout the last 3 years. They have become like a second family to me over the years and I truly appreciate all their encouragement.

I would also like to thank my friends and fellow members of the Kofinas Laboratory. They made my life in graduate school way more fun than and should have been. Finally, I would like to thank Jess, whose strength, drive and determination inspire me every single day.

# Table of Contents

Dedication .....	ii
Acknowledgements .....	iii
Table of Contents .....	v
List of Tables.....	viii
List of Figures .....	ix
1 Chapter 1: Motivation and Background.....	1
1.1 Research Motivation .....	1
1.2 In Vivo Hemostasis .....	2
1.2.1 Blood Coagulation Cascade .....	3
1.3 Hemostatic Technology and Product Review.....	8
1.3.1 Biological-Based Hemostatics .....	9
1.3.2 Synthetic Hemostatics .....	14
1.4 Dissertation Outline .....	19
2 Chapter 2: Investigation into the Critical Mechanical and Electrostatic Properties which Influence Factor VII Activation by Charged Polymer Hydrogels in Plasma.....	21
2.1 Introduction.....	21
2.2 Methods .....	23
2.2.1 Materials .....	23
2.2.2 Hydrogel Synthesis .....	24
2.2.3 Characterization .....	25

2.2.4	Dynamic FVII Activation Experiment .....	26
2.2.5	Surface Area Dependence of FVII Activation.....	26
2.2.6	Optimization .....	27
2.2.7	Dynamic Mechanical Analysis .....	27
2.2.8	Factor Deficient and Factor Inhibition Experiment .....	28
2.2.9	TFPI Activity Experiment .....	29
2.2.10	Artificial Plasma Experiment.....	29
2.3	Results .....	30
2.3.1	Characterization .....	31
2.3.2	Dynamic FVII Activation Experiment .....	32
2.3.3	Surface Area Dependence.....	34
2.3.4	Optimization .....	35
2.3.5	Dynamic Mechanical Analysis .....	38
2.3.6	Biological Mechanism.....	42
2.4	Discussion.....	47
3	Chapter 3: Clinical Diagnostic and Animal Experimentation.....	50
3.1	Introduction.....	50
3.2	Materials and Methods .....	51
3.2.1	Materials .....	51
3.2.2	Hydrogel Synthesis .....	51
3.2.3	Sheep Blood Experiments.....	52
3.2.4	In Vivo Animal Experiments .....	52
3.3	Results .....	54

3.3.1	Sheep Blood Experiments.....	54
3.3.2	In Vivo Animal Experiments .....	56
3.4	Discussion.....	62
4	Chapter 4: Contributions and Future Work.....	65
4.1	Contributions .....	65
4.2	Future Work.....	66
	Bibliography.....	68

## List of Tables

**Table 2.1:** Both the linear elastic modulus (calculated between 0 % - 1 % strain) and the strain hardening modulus (calculated between 4 % - 5 % strain) were calculated for all sample compositions used in the Dynamic FVII Activation and TFPI Activity Experiments. The moduli were calculated by fitting a linear regression to the data for each respective region and obtaining the slope. 3 to 5 samples were used for each calculation (n = 3 – 5). .....40

## List of Figures

- Figure 1.1:** Simplified pictorial depiction of the contact activation complex and corresponding FXII activation<sup>1</sup>. .....5
- Figure 1.2:** Simplified pictorial of the blood coagulation cascade. Calcium ( $\text{Ca}^{++}$ ), phospholipids surface (PL)<sup>2</sup>. .....7
- Figure 1.3:** Scanning electron micrograph of a blood clot consisting of platelets and erythrocytes (red blood cells) entrapped in a fibrin matrix<sup>3</sup>. .....8
- Figure 2.1:** Typical coagulate complex (fibrin-hydrogel complex) formed after rotating a specific hydrogel composition (1.5 M APM, 1.5 M acrylamide, 0.3 M BIS) in human plasma (4 % (w/v) sodium citrate) for 18 hours. 300 mg of dried hydrogel were placed in 9 mL of plasma. ....31
- Figure 2.2:** (A) IHC stained micrograph image of coagulate complex. (B) H&E stained micrograph image of coagulate complex. Polymer hydrogel appears as lighter, smoother material on right side of the micrograph while fibrin appears as the darker, rougher material on the left side of them micrograph. (C) ESEM surface image of the coagulate complex. ....32
- Figure 2.3:** Factor VIIa concentration was measured in citrated human plasma containing various hydrogel compositions at 30, 90, and 180 minutes (left axis: bar

graph). The amount of fibrin formation was also rated for each composition at each time point (right axis: line graph). Data is representative of an average and corresponding standard deviation (error bar) of three (n = 3) separate sample trials. Asterisk (\*) indicates duplicate sample point. ....33

**Figure 2.4:** Factor VIIa concentration was measured in human plasma containing various particle sizes of a hydrogel capable of inducing FVII (composition C from above Dynamic FVII Activation Experiment) and a negative control (HEM Control) at 30, 90, and 180 minutes. Data is representative of an average and corresponding standard deviation (error bar) of three (n = 3) separate sample trials. Asterisk (\*) indicates duplicate sample point. ....35

**Figure 2.5:** Experiment aimed to investigate the effect that various compositional factors including total monomer concentration (acrylamide + APM + BIS), positive electrostatic charge (APM), and cross-linker ratio (acrylamide:APM:BIS) had on fibrin formation (FVII activation). Acrylamide concentration is located on the horizontal axis while APM concentration is on the vertical axis. BIS concentration is also indicated on the horizontal axis and is kept constant for each respective acrylamide concentration. The amount of fibrin formation induced by each composition was visually scored from 0 (no fibrin formation) to 10 (substantial fibrin formation). Images of representative fibrin formation (clot) ratings 0, 2, 4, 6, 8, and 10 are displayed underneath the rating scale for visual reference. All samples were run in triplicate (n = 3). ....36

**Figure 2.6:** Graph of loss modulus vs. frequency of three compositions used in the Dynamic FVII Activation Experiment ranging from high APM, low acrylamide and BIS content (composition A) to low APM, high acrylamide and BIS content (composition F). Spectra for sample compositions C and F are shifted vertically to avoid overlapping of data. Spectra are representative of data obtained from several samples (n = 3 – 5). .....39

**Figure 2.7:** Stress-strain graph of all sample compositions used in the Dynamic FVII Activation Experiment. Curves are representative of data obtained from several samples (n = 3 – 5). .....40

**Figure 2.8:** Optimum hydrogel composition (Composition C from above Dynamic FVII Activation Experiment) tested in various factor deficient and factor inhibited plasmas for 18 hours. After the 18 hour cycle the coagulate complex was drained of plasma, and visually scored for fibrin formation on a scale of 0 (no fibrin formation) to 10 (substantial fibrin formation). All samples were run in triplicate (n = 3). .....43

**Figure 2.9:** TFPI Activity was measured in human plasma containing various hydrogel compositions at 30, 90, and 180 minutes (left axis: bar graph). The amount of fibrin formation was also rated for each composition at each time point (right axis: line graph). Data is representative of an average and corresponding standard

deviation (error bar) of three (n = 3) separate sample trials. Asterisk (\*) indicates duplicate sample point. ....46

**Figure 2.10:** (A) Image of hydrogel capable of inducing optimum FVII activation, Composition C used in previous experimentation, (orange cap), along with a HEM control hydrogel (blue cap) and a blank control (red cap) after 30 minute rotation in artificial plasma explicitly lacking calcium, tissue factor (TF), and platelets. Arrow shows fibrin clot formation. Artificial plasma consisted of 137 nM NaCl, 2.7 mM KCl, 0.4 mM sodium phosphate monobasic, 5.5 mM dextrose, 10 mM HEPES, 0.5 µg/mL FVII, 10 µg/mL FX, 100 µg/mL FII<sup>31</sup>, 7 µg/mL FV<sup>32</sup>, 5 µg/mL FIX, 2.6 mg/mL FI, and 30 µg/mL FXIII. (B) IHC stained image of clot formation observed with Composition C. ....47

**Figure 3.1:** Clot formations induced by the hydrogel compared to a blank control. Approximately 1 mL of sheep blood, drawn directly from the animal, was added to a glass vial containing 250 mg of polymer hydrogel (2.73 M APM, 0.27 M acrylamide, and 0.054 M BIS) along with a blank glass vial. Clot formation was induced by the hydrogel in approximately 2 minutes compared to clot formation observed in the blank control which took over 10 minutes. ....55

**Figure 3.2:** Image of lung incision site before hydrogel is applied (A), during the application of the hydrogel (B), and after the hydrogel is removed (C). ....58

**Figure 3.3:** Optical micrographs of H&E stained sections of the lung incision site. Magnifications of 5x (A), 10x (B), and 20x (C). .....59

**Figure 3.4:** Image of the initial liver incision site, before hydrogel is applied (A). Image of same site after the hydrogel is removed (B). Complete hemostasis was observed in 5 minutes. ....60

**Figure 3.5:** H&E stained micrographs of the liver incision site. ....61

**Figure 3.6:** Carstairs' Method stained micrographs of liver incision site. Fibrin (red-orange), collagen (blue), erythrocytes (red-yellow), platelets (grey). ....61

# 1 Chapter 1: Motivation and Background

The overarching goal of this research is a better understanding of how polymer hydrogel morphology, mechanical properties and electrostatic charge interact with and affect the body's hemostatic response. The directed goal of the research is translating this understanding into the development of a new polymer hydrogel-based material for hemorrhage control.

## 1.1 Research Motivation

Traumatic injury is the leading cause of death worldwide for persons between the ages of 5 and 44, accounting for over 5,000,000 deaths each year<sup>4</sup>. Uncontrolled hemorrhaging, or blood loss, accounts for 30 % to 40 % of these deaths and is the leading cause of preventable deaths after hospital admission. Moreover, on the battlefield an astounding 90 % of deaths occur before soldiers reach critical care, mainly due to blood loss<sup>2-4</sup>. Furthermore, there are over 500,000 people around the world living with potentially lethal clotting disorders such as hemophilia.

There are two main categories of hemostatic materials used to control hemorrhaging: biological-based and synthetic. Biological-based hemostatics, which contain animal derived or purified human clotting substrates such as thrombin or fibrin, are quite effective at controlling blood loss but carry serious disease transmission risks and are prohibitively expensive for people in developing countries where over 90 % of these deaths are occurring<sup>5</sup>. Synthetic-based hemostatics are less expensive yet not nearly as effective as their biological counterparts at effectively

controlling blood loss. It is only through a better understanding of how materials interact with the body's hemostatic response will we as engineers be able to design materials capable of safely and effectively amplifying this response to control life threatening blood loss. The advancement of hemostatic technology, and the development of an inexpensive and effective material capable of rapidly stopping blood loss, has the potential to save millions of lives each year.

## **1.2 In Vivo Hemostasis**

The body's hemostatic response to control blood loss involves two distinct processes: a primary response involving the formation of a platelet-based seal at the wound site, and a secondary response which involves the activation of the coagulation cascade resulting in the stabilization of this platelet plug by fibrin. The initial stage in the primary hemostatic response is marked by the adhesion and deposition of platelets to collagen within the subendothelium layer of the wound site. The adhesion of platelets to the injured vessel wall is mediated by the binding of von Willebrand Factor (vWF) to several distinct platelet glycoprotein receptors, most notably Ib-V-IX and integrin  $\alpha_{IIb}\beta_3$ <sup>6</sup>. Besides glycoprotein Ib, there are several other immunoglobulin collagen receptors on the platelet surface which are also capable of providing tethering to the subendothelium at the wound site, including glycoproteins Ia/Ia, IV, VI, p47, and p65<sup>7-9</sup>.

Binding of vWF also initiates the activation of platelets. Initial activation of platelets causes them to transform in shape from smooth discoids to "spiny" spheroids projecting long pseudopodia tentacles. Activation also induces platelets to release the

contents of their main storage units;  $\alpha$ -granules which contain thrombospondin, fibrinogen, fibronectin, platelet factor 4, vWF, platelet-derived growth factor,  $\beta$ -thromboglobulin, Factor V (FV), and FVIII, along with dense bodies which contain adenosine diphosphate (ADP), adenosine triphosphate (ATP), and serotonin<sup>10</sup>. These molecules are key to initiating further platelet activation and aggregation resulting in the formation a hemostatic platelet plug at the wound site. Platelet activation also induces the exposure of negatively charged surfaces on platelet membranes which facilitate the activation of the coagulation pathway. Activation of the coagulation pathway results in the generation of fibrin which stabilizes initial platelet plug formation (secondary hemostasis). The rapid generation of fibrin at the wound site is crucial to stabilizing the initial platelet plug to control hemorrhaging.

### **1.2.1 Blood Coagulation Cascade**

The blood coagulation cascade is a remarkably complex biological process which has evolved over millions of years. This evolution has led to the development of an incredibly intricate yet coordinated system consisting of various components which interact in incredibly specific ways to yield a single final product; fibrin. The evolutionary complexity of the system is simultaneously its greatest strength, allowing for feedback regulation on a multitude of levels, and its greatest weakness, introducing more proverbial links in the chain which may ultimately fail. Yet it was through the discoveries of these supposed weak links which has led to most of our modern understanding of the functioning of the blood coagulation cascade. In 1936 researchers discovered that patients with hemophilia lacked a clotting protein

necessary for proper clotting, which was later termed factor VIII (FVIII)<sup>11</sup>. The study of individuals with deficiencies in their clotting mechanism led to the discoveries of many other clotting factors including FV<sup>12,13</sup>, FVII<sup>14</sup>, FVIII<sup>11</sup>, FIX<sup>15,16</sup>, FX<sup>17,18</sup>, FXI<sup>19</sup>, and FXII<sup>20</sup>. It is mainly through these discoveries that have led to the modern day understanding of the blood coagulation cascade, yet it apparent from the recent discoveries that this understanding is far from complete.

The blood coagulation cascade involves a series or “cascade” of zymogen activation reactions. At each stage a precursor protein (zymogen) is converted to an active protease by cleavage of one or more peptide bonds in the precursor molecule. The coagulation cascade consists of two pathways: the contact activation pathway, and the tissue factor pathway which lead to the ultimate activation of the final common pathway. The activation of the contact activation pathway, formerly known as the intrinsic pathway, involves the mutual coordination of 4 key proteins which form what is known as the contact complex and consists of FXII, FXI, high molecular weight kininogen (HMWK) and prekallikrein (PK). It is the association of these proteins, in contact with an anionic surface, which leads to the activation FXII and corresponding contact pathway activation. PK, the zymogen of kallikrein, has the capability of inducing the direct activation of FXII and is also involved in the association of HMWK within the contact complex. HMWK is the main cofactor of the complex and contains binding sites for PK, FXI, and calcium along with a domain which is capable of interacting with hydrophilic and anionic surfaces<sup>21-23</sup>. The role of HMWK in the contact activation pathway is related to its ability to coordinate the FXI-PK-FXII complex together resulting in the activation of FXII<sup>24</sup>. Activated FXII

(FXIIa) is able to directly activate FXI (FXIa) in the presence of HMWK which in turn is able to activate FIX (FIXa), an event in which calcium and platelets, or rather a phospholipid surface are primary cofactors. FIXa combines with its primary cofactor activated FVIII (FVIIIa) to form a membrane (phospholipid)-bound complex known as the Xase ternary complex, which results in the direct activation of FX and corresponding common pathway<sup>25,26</sup>.

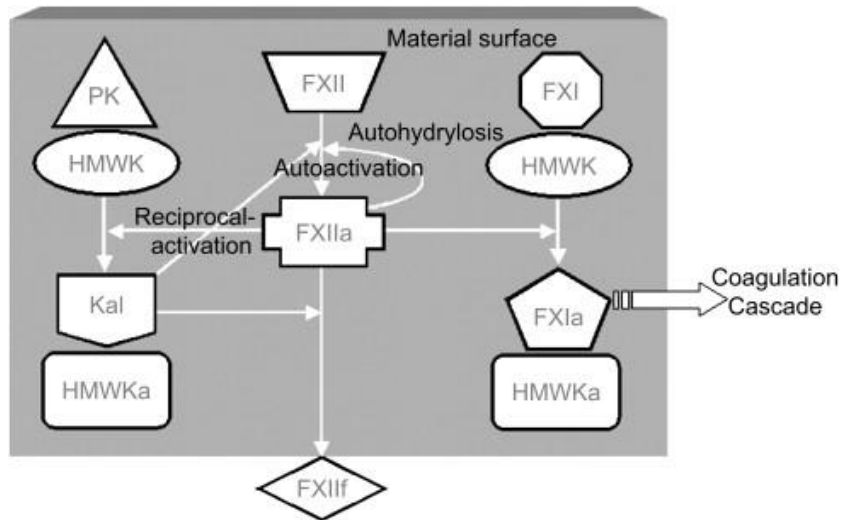


**Figure 1.1:** Simplified pictorial depiction of the contact activation complex and corresponding FXII activation<sup>1</sup>.

Research has recently shown that the tissue factor pathway is the primary pathway of fibrin formation, while the contact activation pathway acts primarily as an amplifier of cascade activation and fibrin generation<sup>27,28</sup>. The activation and sustainment of the tissue factor pathway involves the coordination of a multitude of proteins and cofactors including FVII, calcium, tissue factor pathway inhibitor (TFPI), tissue factor (TF), and a phospholipid surface. Human coagulation FVII is a single chain, glycoprotein which circulates in normal human blood and is the main activator of the tissue factor pathway<sup>29,30</sup>. Cleavage of a single peptide bond results

in a structural change which activates the zymogen transforming it into a potent vitamin K-dependent serine protease. This structural change also allows for the protein to effectively bind to its cofactor, TF. The distribution of TF is carefully coordinated in a hemostatic layer, with the ability to induce coagulation upon the disruption of the vascular endothelium<sup>31-35</sup>. TF forms a stable complex with FVIIa, and this complex is capable of directly initiating the common coagulation pathway via the activation of FX or indirectly through the activation of FIX which in turn is able to activate FX<sup>36</sup>. TF is most effective as a procoagulant when incorporated into phospholipid membranes, a surface which is typically provided by platelets<sup>37-39</sup>.

Calcium has been shown to play a key role as a cofactor in the generation and activity of several vitamin K-dependant serine protease coagulation factors, including FVIIa<sup>40,41</sup>. A high-affinity calcium binding site in the protease domain of FVII has been shown to mediate the interaction between TF and FVIIa<sup>41,42</sup>. Conversely, the  $\gamma$ -carboxyglutamic acid (Gla) domain of FVIIa contains several low affinity calcium binding moieties which aid in the interaction of FVIIa and phospholipid surfaces<sup>43</sup>. In most instances, calcium binding leads to a necessary conformation change which allows these factors to effectively “dock” on a surface and exhibit their cleavage site. Without the binding of calcium, in calcium depleted medium, it is believed that this Gla domain slightly unfolds exposing a highly negatively charged domain to the media which is capable of interacting with a positively charged surface. Although groups have shown the capability of FVII to bind to such positively charged surfaces in calcium depleted environments, such as citrated plasma, the mechanism by which this occurs, specifically the material properties which affect this process, are not well

understood. TFPI is the main inhibitor of the FVIIa-TF complex, and is an important feedback regulator of tissue factor pathway activation<sup>44,45</sup>.

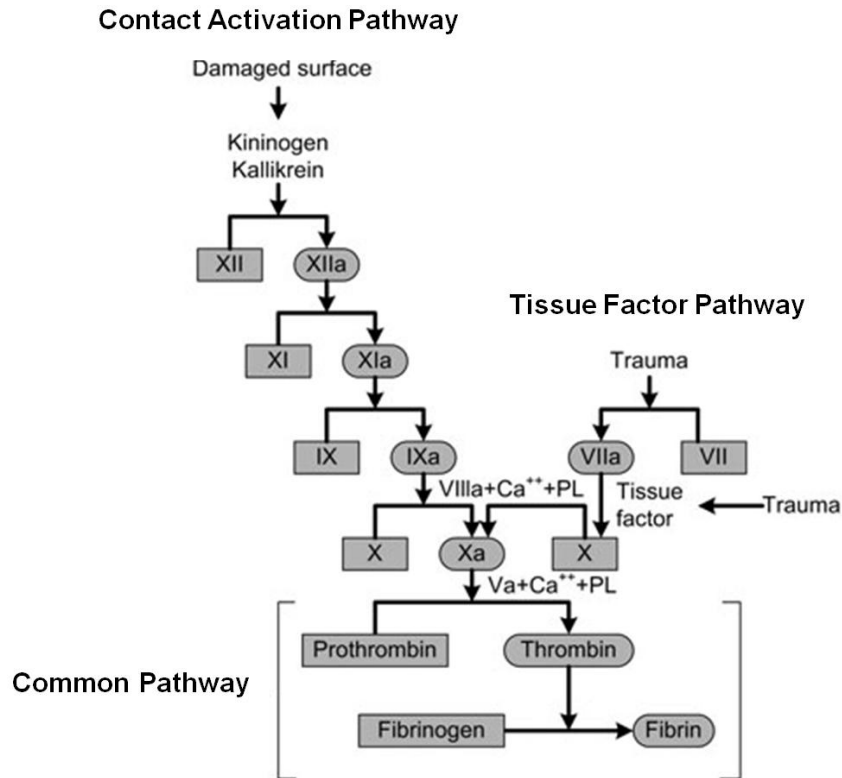


**Figure 1.2:** Simplified pictorial of the blood coagulation cascade. Calcium (Ca<sup>++</sup>), phospholipids surface (PL)<sup>2</sup>.

The activation of FX by either FIXa or the FVIIa-TF is the initial step in the activation of the final common pathway. Immediately after activation FXa complexes with FVa to form a complex, known as the prothrombinase complex, which is capable of converting the zymogen prothrombin (FII) to its enzymatic analogue thrombin (FIIa). The ability of this prothrombinase complex to convert prothrombin to thrombin is highly dependent on both calcium and a phospholipid surface, which is typically provided by platelets. Thrombin catalyzes a multitude of key reactions including platelet activation, activation of FV, FVIII, FXI, and FXIII

along with directing the disassociation of FVIII from vWF, and the conversion of fibrinogen to fibrin. Although the initial amount of thrombin formation is unable to produce a sufficient amount of fibrin to stabilize the formed platelet plug, the reactions it sets in place in combination with the sustained activation of FX lead to a subsequent thrombin burst which results in substantial fibrin formation<sup>46</sup>. Fibrin strands form spontaneously after conversion, which are subsequently cross-linked by FXIIIa resulting in a matrix which entrap platelets and erythrocytes (red blood cells) to produce a stabilized hemostatic plug at the wound site (Figure 1.3).

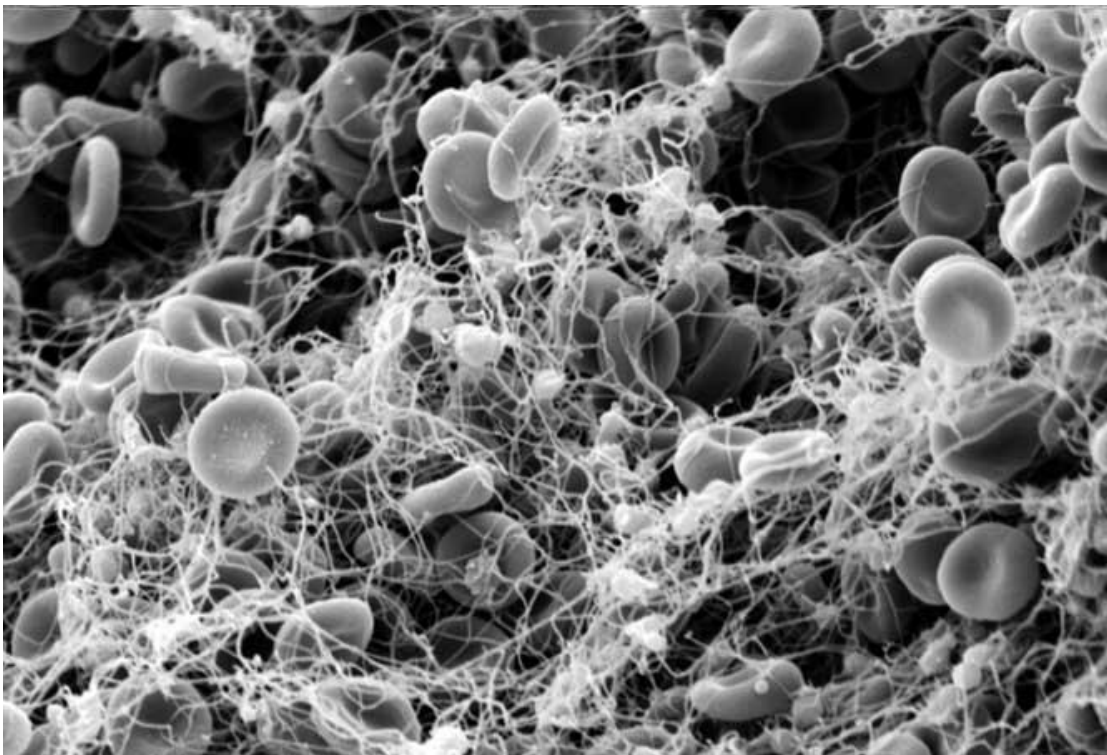


**Figure 1.3:** Scanning electron micrograph of a blood clot consisting of platelets and erythrocytes (red blood cells) entrapped in a fibrin matrix<sup>3</sup>.

### **1.3 Hemostatic Technology and Product Review**

The field of hemostatic agents and materials has expanded dramatically within the last century. The current worldwide hemostatic market of U.S. is reported to be

around \$700 million and is expected to reach \$1.5 billion by 2015. This considerable expansion and evolution of the field throughout the last century has also been accompanied by tremendous diversification resulting in a multitude of hemostatic products now available on the market, each with their own advantages and disadvantages.

The hemostatic products available on the market today are either biological-based or synthetic. Biological-based hemostatics are defined as any hemostatic agent comprised of animal or “animal derived” substrates. These types of hemostatic agents typically work by initiating, amplifying, or assisting the natural coagulation system. Although they have excellent hemostatic effects and work via the promotion of the body’s natural responses, they are incredibly expensive (up to \$500 per application) and carry risks of disease infection and severe immunological response. Synthetic hemostatic agents are typically less expensive yet often fail to effectively induce hemostasis and are mainly designed to be scaffolds for coagulation to occur. Furthermore, most biological and synthetic hemostatic materials are dependent on clotting platelets to achieve their effect, making them ineffective with patients with platelet deficiencies, such as thrombocytopenia. Additionally, there are virtually no hemostatic agents with the capability of delivering therapeutics in a controlled and efficient manner.

### **1.3.1 Biological-Based Hemostatics**

Biological-based hemostatic agents contain, incorporate, or are derived from animal (biological) substrates, i.e. proteins, or cells. They can further be subdivided

into the type of biological substrates incorporated into the system including collagen, thrombin, fibrin, albumin, and/or platelets.

### **1.3.1.1 Collagen**

Collagen is the main protein of connective tissue in mammals, including the skin, bones, ligaments, and tendons making up about 30 % of the total protein in the body<sup>47</sup>. In addition to providing structural integrity for the animal body, including all organs, collagen also facilitates the activation of the coagulation cascade. Collagen's ability to facilitate coagulation, along with the fact that it is naturally occurring, makes it an ideal choice for a hemostatic agent. Collagen is typically incorporated into the products via gelatin or microfibrillar form. Gelatin is an irreversibly hydrolyzed form of collagen and may be prepared as a powder, sponge, sheet, film or foam. Gelatin products are typically pliable, easy to handle, and relatively inert. When placed in soft tissue gelatin products typically absorb in 4 to 6 weeks, yet when applied to bleeding nasal, rectal or vaginal mucosa, will liquefy in approximately 2 to 5 days. The product *Gelfoam* (Pfizer, New York, NY), first introduced in 1945, is produced from purified pork skin gelatin granules. Effects appear to be more physical than the result of altering the blood clotting mechanism. The foam swells up to 45 times its original dry weight and 200 % of its initial volume.

Microfibrillar collagen is the predominant form used in modern hemostatic products. The collagen network acts as a framework which aggregates clotting factors, platelets, along with various coagulative and adhesive proteins to facilitate clot formation. The product is typically formed into various products including

powder (shredded fibrils), sheets, and sponges. Market examples include *Ultrafoam* (Davol Inc., Cranston, RI), *Avitene* (Davol Inc., Cranston, RI), *Instat* (Johnson & Johnson, Langhorne, PA), *Helistat* and *Helitene* (Integra LifeSciences, Plainsboro, NJ), *Collatape/CollaCote/CollaPlug* (Integra Lifesciences Corporation, Plainsboro, NJ), *Collastat* and *Collatene* (Xemax, Napa, CA)<sup>48</sup>.

Collagen-based hemostatic products are easily removable, cause little aggravation to the wound site, and can be very effective at controlling hemorrhaging (especially relative to cellulose or gelatin-based hemostatics)<sup>48</sup>. Disadvantages of collagen-based products include their high price (around \$150 per dressing), poor biodegradability, inherent risk of antigenicity, low solubility (difficult to make concentrated solutions), and handling difficulties since the products will irreversibly adhere to any hydrated surface<sup>48,49</sup>.

### **1.3.1.2 Thrombin**

Thrombin is the central activating enzyme of the common coagulation pathway. Thrombin circulates within blood in its precursor (zymogen) form, prothrombin. Prothrombin is specifically cleaved to produce the enzyme thrombin. The main role of thrombin in the coagulation pathway is to convert fibrinogen into fibrin, which in turn is covalently cross-linked to produce a hemostatic plug. Thrombin products are typically sold in liquid or powder form and include *Thrombostat* (Parke-Davis, Ann Arbor, MI), *Thrombin-JMI* (King Pharmaceuticals, Bristol, TN), and *Quixil* (Omrrix Biopharmaceuticals Ltd, Tel Hashomer, Israel). There are also several combination products which include *Evicel* (Johnson & Johnson, Langhorne, PA) which is a

combination of thrombin and fibrin used mainly as a tissue sealant, along with *FloSeal* and *SurgiFlow* (Baxter Healthcare Corporation, Westlake Village, CA) which are both hybrid products composed of bovine or porcine gelatin and thrombin<sup>48</sup>.

Thrombin products take advantage of the natural physiologic coagulation response by augmenting, amplifying, and assisting the process. Advantages of thrombin-based products include low risk of foreign body or inflammatory reactions, firm attachment to wound bed, and its excellent hemostatic effect, specifically with patients that have platelet dysfunctions<sup>50</sup>. Another advantage of thrombin is the versatility that the product may be applied, in powder or liquid (spray on) form. Disadvantages of these products include their often prohibitive high price (\$75 - \$500 per application), difficulty of use including the inconvenience of premixing preparation, along with the risk of intravenous introduction which may result in intravascular clotting<sup>48,50</sup>.

### **1.3.1.3 Fibrin**

Fibrin is a fibrillar protein which is polymerized and cross-linked to form a mesh network, typically at the site of an injury after the induction of the coagulation cascade. The mesh network, incorporative of other various proteins and platelets, forms a hemostatic plug to prevent continuous or further blood loss<sup>51</sup>. Fibrin is converted from fibrinogen by thrombin. Fibrin is in turn polymerized and covalently cross-linked by FXIIIa<sup>52</sup>. Due to its natural mechanical hemostatic role fibrin has been commercially used to control blood flow since the early 1900s<sup>53</sup>. Most fibrin

glues or fibrin sealants are derived from human and bovine tissue. The product is typically sold in a dual syringe. The first syringe compartment contains the matrix and matrix stabilizing components including fibrinogen, FXIII, fibronectin, and fibrinolysis inhibitors. The second syringe compartment contains the activating agent, typically thrombin and calcium chloride. At the time of application, the contents of both syringes are ejected, combining to activate fibrin matrix formation which typically takes a matter of seconds to set and approximately 5 to 10 days to degrade or absorb into the body. Various fibrin sealants on the market include *Tiseel* (Baxter HealthCare Corporation, Westlake Village, CA), *FibRx* (CryoLife Inc., Kennesaw, GA), *Crosseel* (Johnson & Johnson, Langhorne, PA), *Hemaseel* (Haemacure Corporation, Montreal, Quebec), *Beriplast P* (Aventis Behring, King of Prussia, PA), and *Bolheal* (Kaketsuken, Kumamoto, Japan)<sup>48</sup>.

Fibrin-based hemostatics or tissue sealants are fast acting, composed of native coagulative factors, are biodegradable, do not promote inflammation or tissue necrosis, have diverse applications, and are particularly useful in patients with coagulation deficiencies such as hemophilia or von Willebrand's disease. Major disadvantages of these products include their often prohibitive price (\$100 - \$300/mL), their fragile nature, and difficulty of handling and application<sup>48,54</sup>.

#### **1.3.1.4 Other Biological-Based Hemostatics**

Other prominent biological-based hemostatic products include those composed of covalently cross-linked protein networks such as *BioGlue* (Cryolife, Kennewsaw, GA), along with products which incorporate platelets such as *Costasis*, marketed as

*Vitagel* (Orthovita, Malvern, PA). BioGlue is comprised of bovine serum albumin, and various other proteins, cross-linked with glutaraldehyde to form a rigid, insoluble matrix. The reaction occurs spontaneously upon the introduction of glutaraldehyde to the protein mixture, and requires no external factors such as coagulation factors<sup>55</sup>. Disadvantages of these products include their high price (\$300 - \$425/ml application), mediocre hemostatic effect<sup>56</sup>, necessity of a dry environment for application<sup>55</sup>, the toxic effects associated with tissue exposure to glutaraldehyde<sup>57</sup>, and risk of immune reactions associated with glutaraldehyde-based products<sup>58</sup>.

*Costasis* is a combination product combining bovine collagen and the patient's own platelets. The collagen within the product promotes fibrin-induced hemostasis on its network<sup>48,59</sup>. The presence of platelets in such a product improves overall clot strength and supplies various growth factors which facilitate tissue regeneration. Disadvantages include high price (\$100 - \$150/mL) and difficulty of application<sup>48</sup>.

### **1.3.2 Synthetic Hemostatics**

Non biological-based, or synthetic, hemostatic agents are defined as any product which does not incorporate biological materials, or more specifically animal derived components. Synthetic hemostatics are typically cheaper, easier to use, and easier to apply relative to their biological counterparts. Furthermore, synthetic hemostatics have no innate antigenicity, rarely induce immune responses or inflammatory reactions, and are inherently free of disease vectors<sup>60</sup>. The main classes of synthetic hemostatic include cyanoacrylates, polysaccharides (e.g. oxidized cellulose, N-acetyl glucosamine), synthetic polymers, and mineral/metal based.

### 1.3.2.1 Cyanoacrylates

Cyanoacrylates are liquids that rapidly polymerize. These products create a tight seal between tissues, obstructing blood flow. Cyanoacrylates are categorized upon their length. Shorter chain cyanoacrylates (ethyl cyanoacrylates) are typically quicker to absorb yet more toxic relative to intermediate (butyl cyanoacrylates) or longer chain cyanoacrylates (octyl cyanoacrylates)<sup>61</sup>. Due to their inherent high toxicity few hemostatic products composed of short chain cyanoacrylates have reached the market. There is however some research supporting the efficacy of *Krazy Glue* (ethyl-2-cyanoacrylate, Elmer's, Columbus, OH) for cutaneous wound closure<sup>62</sup>. Cohera Medical Corporation is currently in the process of developing a butyl cyanoacrylate (isobutyl-2-cyanoacrylate), marketed as *TissuGlu* (Cohera Medical Inc., Pittsburgh, PA). Furthermore, there are several octyl acrylate-based hemostatic products that are FDA-approved for skin closure which include *Dermabond* (Ethicon, Somerville, NJ) and *Band-Aid Liquid Bandage* (Johnson & Johnson, Langhore, PA).

Cyanoacrylates are typically nonreactive, do not promote infection, rapidly curing, and are only moderately expensive<sup>48</sup>. Disadvantages of cyanoacrylates and cyanoacrylate-based hemostatics include difficulty of application due to their highly adhesive nature, and risk of tissue neurotoxicity, fibrosis and inflammatory reactions<sup>50</sup>.

### 1.3.2.2 Polysaccharides

The two main polysaccharides used as hemostatics today are oxidized cellulose and poly-N-acetyl glucosamine. The hemostatic effects of certain polysaccharides,

specifically oxidized cellulose and N-acetyl glucosamine, have been known since the early twentieth century. Oxidized cellulose is derived from plant fiber, which is in turn oxidized in the presence of nitrogen dioxide to form cellulosic acid<sup>63</sup>. Oxidized cellulose has been shown to accelerate thrombin generation within the body<sup>64</sup>. Furthermore, the polysaccharide meshwork serves as a physical framework for coagulation to occur, with moderate absorbent properties<sup>50</sup>. Oxidized cellulose products on the market today include *Oxycel* (Becton Dickinson, Franklin Lakes, NJ), *Celox* (Medtrade Products Ltd., Crewe, England), *Surgicel* (Johnson & Johnson, Langhorne, PA), and *BloodStop* (LifeScience PLUS, Inc., Santa Clara, CA).

Cellulose-based hemostatics are relatively easy to handle, fully absorbable and biodegradable (over 1 to 6 weeks), relatively inexpensive, and have antibacterial properties<sup>65</sup>. The major drawback of these products is the risk of foreign body reactions<sup>66,67</sup>. Furthermore, these products have only moderate hemostatic capability and therefore are reserved as an adjunct to the body's natural clotting response rather than a synthetic replacement.

Poly-N-acetyl glucosamine, also known as chitin or chitosan, is a complex polysaccharide produced by fermenting microalgal cultures. The hemostatic effects of poly-N-acetyl glucosamine are believed to be a result of the attraction and binding of circulating blood cells<sup>68</sup>. The positive charges on the polymer attract the negatively charged erythrocytes to help seal the clot. Poly-N-acetyl glucosamine also induces vasospasm effects which aid in hemostasis<sup>68</sup>. Poly-N-acetyl glucosamine products include *HemCon* (HemCon Inc., Portland, OR), *TraumaDex* (Medafor, Minneapolis, MN), *SyvekPatch* (Marine Polymer Technologies Inc., Danvers, MA),

*Clo-Sur P.A.D.* (Scion Cardio-Vascular, Miami, FL), and *Chito-Seal* (Abbott Vascular Devices, Redwood, City, CA)<sup>48</sup>.

Advantages of poly-N-acetyl glucosamine dressings include their ease of application, robustness, and lack of toxicity. Disadvantages include the high cost (\$100 per unit) and variability of efficacy between batches<sup>68</sup>.

### **1.3.2.3 Synthetic Polymers**

Most polymer-based hemostatics are designed to provide a mechanical tissue sealant. The majority of products on the market today are composed of polyethylene glycol (PEG) which are applied and polymerized at the wound site. The polymer is typically cross-linked with itself or with a primer to yield a robust framework stopping blood flow and sealing tissue. Most PEG products undergo biodegradation in approximately 30 days. PEG products include *Coseal* (Baxter Healthcare Corporation, Westlake Village, CA) and *AdvaSeal-S* (Genzyme Corporation, Cambridge, MA). PEG-based hemostatics or tissue sealants are typically non-inflammatory, do not induce immune response, and are biodegradable. Drawbacks include difficulty of application and high price (\$200/application).

Pro QR Powder (Bioline, Sarasota, FL) is another polymer-based hemostatic on the market today. Pro QR is a combination product of a hydrophilic polymer and a potassium iron oxyacid salt. The polymer is absorptive of blood flow, promoting the formation of a natural blood clot while the potassium salt component releases iron which complexes with proteins and activates hemostatic channels<sup>48,69</sup>. The product is

inexpensive, nontoxic, easily stored, flexible, stops bleeding rapidly, and is available over the counter. The main drawback of the product is its awkward application<sup>48</sup>.

#### **1.3.2.4 Mineral/Metal**

The final class of non-biological, or synthetic, hemostatics includes those which incorporate metal salts or minerals such as zinc, iron, silver nitrate, or aluminum chloride. Although this class of hemostatics are typically easy to use, cost-effective, and provide adequate hemostatic effects their toxic side effects limit their appeal.

Zinc paste was first used to fix tissue after surgery in the early 1940s. Zinc paste solutions have impressive hemostatic abilities but are rarely used do to their harmful side effects including pain and toxicity at the site<sup>50</sup>. Monsel's solution is a 20 % ferric subsulfate solution, which is believed to occlude vessels via protein precipitation. Monsel's solution is easy to obtain, cost-effective, and resistant to bacterial contamination. Major disadvantages include its caustic and toxic nature which may promote melanocyte activity, increased erythema, dermal fibrosis, and reepithelialization<sup>70,71</sup>. Silver nitrate is typically used as a 10 % solution and coagulates blood through protein precipitation. Silver nitrate is cost-effective, easy to use, and has potent antibacterial properties. Disadvantages include its severe tissue toxicity, risk of permanent skin discoloration, and the painful burning sensation experienced upon application. Aluminum chloride has modest hemostatic properties and is prepared in concentrations of 20 % to 40 % in water, alcohol, ether, or glycerol. Its mechanism of action is thought to be caused by the hydrolysis of the salt, resulting in the generation of hydrogen chloride which causes vasoconstriction,

and can assist in the activation of the tissue factor, or extrinsic, coagulation pathway<sup>50,48</sup>. Aluminum chloride is cost effective, easy to use, and may be stored at room temperature. Side effects of its use include painful paresthesia, tissue irritation, and reepithelialization. Aluminum chloride solutions are marketed as *Drysol* and *Xerac AC* (person-Covey, Dallas, TX)<sup>48</sup>.

A small subclass of hemostatics is based upon various mixtures of minerals. Zeolite is a granular mixture of silicon, aluminum, sodium, and magnesium derived from lava rock. When coming into contact with blood the mixture absorbs water, concentrating platelets and coagulation factors within the wound, accelerating the clotting process. Zeolites have also been shown to induce the potent activation of the contact activation pathway, via the activation of FXII. QuikClot (Z-Medica, Wallingford, CT) is the main product which is based upon a zeolite mixture. Zeolite is inexpensive, easy to manufacture, clots fairly quickly, robust under various conditions, and is fairly immunological inert<sup>48</sup>. The main drawback of the formulation is the risk of thermal injury associated with use.

## **1.4 Dissertation Outline**

This research has focused on a better understanding of how material properties of a polymer hydrogel, specifically positive electrostatic charge and mechanical stiffness, effect the body's clotting response. Initial in vitro research focused on investigating the key material properties which affect the activation of the coagulation cascade, specifically FVII, in calcium depleted plasma (Chapter 2). Subsequent clinical diagnostic experimentation was conducted to determine the key material

properties which affect primary hemostasis, i.e. platelet plug formation, in vivo (Chapter 3). Live animal testing was also completed to further investigate the effect that electrostatic charge and mechanical stiffness has on in vivo hemostasis and also to determine the viability of such a polymer hydrogel to control hemorrhaging in a clinically relevant model. The specific goal of this research was a better understanding of the interactions that occur between polymer hydrogels and the body's clotting response for the directed development of an inexpensive, safe, and effective hemostatic material.

## **2 Chapter 2: Investigation into the Critical Mechanical and Electrostatic Properties which Influence Factor VII Activation by Charged Polymer Hydrogels in Plasma**

### **2.1 Introduction**

There has been considerable research into the effects of charged surfaces on the blood coagulation cascade. The ability of negatively charged surfaces, such as glass or the mineral kaolin, to initiate the contact activation pathway via activation of FXII has been known for over 50 years<sup>72,73</sup>. Recently, research has shown that negatively charged polyphosphate species are capable of enhancing fibrin clot structure<sup>74</sup>. It had previously been discovered by Bjourn et al.<sup>75</sup>, that highly positively charged materials have the ability to activate FVII. Later research by Pederson et al.<sup>76</sup>, explained the ability of these positively charged surfaces to activate FVII via an auto-activation theory. Other research groups have shown that amine containing polymers such as poly(lysine) are capable of enhancing the activation of FX along with FII<sup>76-82</sup>.

Although the ability of charged surfaces to induce specific coagulation factor activation is well known, the roles that specific material properties have in the activation is not well understood. Research was conducted to help establish a better understanding of the effects that material properties, specifically the combination of electrostatic charge and mechanical rigidity, have on the ability of a synthetic polymer-based material to induce the activation of FVII in citrated human source plasma. Plasma was chosen to investigate the activation of FVII since it does not contain cellular species such as erythrocytes and platelets which considerably

complicate the analyses. Subsequent experimentation looked to translate the results obtained using plasma to blood in clinical diagnostic experimentation.

Although FVIIa therapy is quite effective at controlling various types of hemorrhaging, the treatment is often prohibitively expensive and carries serious thromboembolic risks due to its systemic exposure<sup>83,84</sup>. FVIIa requires tissue factor (TF) in order to effectively induce the activation of FX (common pathway). Since TF is only exposed in area of vascular disruption, i.e., hemorrhaging, the hemostatic effect of the material is confined to this area and would not have the inherent risk of inducing thrombus formation within the vasculature, unlike kaolin-based materials. Based on known dynamics of in vivo hemostasis, activation of the tissue factor pathway should elicit clot formation much more rapidly than products based on contact pathway activation, i.e., FXII activation. Contrary to products which activate FXII (such as kaolin-based products), a material capable of inducing FVII activation does not rely on FVIII and FIX, factors which are lacking in patients suffering from hemophilia A and B. In a broader sense, the research aimed to establish a better understanding of the interactions occurring between a synthetic polymer and the blood coagulation cascade, which will be integral in the future development of blood contacting devices.

## 2.2 Methods

### 2.2.1 Materials

Acrylamide, N,N'-methylenebisacrylamide (BIS), N,N,N',N'-tetramethylethylenediamine (TEMED), 4-(2-Hydroxyethyl)piperazine-1-ethanesulfonic acid (HEPES), ammonium persulfate (APS), and human fibrinogen (FI) were purchased from Sigma-Aldrich (Milwaukee, WI). N-(3-aminopropyl)methacrylamide hydrochloride (APM) was purchased from Polysciences (Warrington, PA). N-(2-hydroxyethyl)methacrylamide (HEM) was purchased from Monomer-Polymer (Trevose, PA). Sodium hydroxide (NaOH), sodium phosphate monobasic, sodium chloride (NaCl), potassium chloride (KCl), and hydrochloric acid (HCl) were purchased from Mallinckrodt Baker (Phillipsburg, NJ). Dextrose (anhydrous, ACS grade) was purchased from EMD Chemicals (Madison, WI). Deionized water (DI water) was obtained using a Millipore Super-Q water system (Billerica, MA). Plastic capped glass vials were purchased from VWR Scientific (West Chester, PA). 24-well cell culture plates were purchased from Corning Life Science (Corning, NY).

Normal, human source plasma (pooled, sterile filtered, 4 % (w/v) sodium citrate) and factor I (FI) deficient plasma (pooled, sterile filtered, 4 % (w/v) sodium citrate) were purchased from Vital Products (Boynton Beach, FL). Human FI (fibrinogen) was purchased from Sigma-Aldrich (Milwaukee, WI). Human coagulation factor II (FII), FV, FVII, FIX, and FX were purchased from Haematologic Technologies (Essex Junction, VT). All proteins were buffered in 50 % (v/v) glycerol/water. FII deficient plasma, FV deficient plasma, FVII deficient plasma, FVIII deficient plasma,

FIX deficient plasma, FX deficient plasma, FXI deficient plasma, and FXII deficient plasma along with the chemical inhibitors corn trypsin inhibitor (CTI), D-phenylalanyl-L-prolyl-L-arginine chloromethyl ketone (PPACK), and L-glutamyl-L-glycyl-L-arginine chloromethyl ketone (GGACK) were all purchased from Haematologic Technologies (Essex Junction, VT). All factor deficient plasmas were prepared from citrated (4 % (w/v) sodium citrate), normal human plasma (pooled, sterile filtered). Goat polyclonal primary fibrinogen antibody was purchased from Abcam (Cambridge, MA). The immunogen of this antibody was fibrinogen of human plasma (Abcam, ab6666). Alexa Fluor 488 labeled donkey anti-goat IgG antibody was purchased from Invitrogen (Carlsbad, CA).

### **2.2.2 Hydrogel Synthesis**

A specific amount of either acrylamide, N,N'-methylenebisacrylamide (BIS), N-(2-hydroxyethyl)methacrylamide (HEM), or N-(3-aminopropyl)methacrylamide hydrochloride (APM) was dissolved in DI water and mixed thoroughly until all components were completely solvated. The solution was then titrated to a pH between 6.8 and 7.2 using sodium hydroxide (NaOH) and/or hydrochloric acid (HCl). After pH adjustment, the monomer solution was initiated by adding 20  $\mu\text{L}/\text{mL}$  of a 7.5 % (v/v) N,N,N',N'-tetramethylethylenediamine (TEMED) solution, followed by adding 20  $\mu\text{L}/\text{mL}$  of a 15 % (w/v) solution of ammonium persulfate (APS), for polymerization. After polymerizing overnight, all polymer hydrogels were dried in a vacuum (85 kPa) oven at 85 °C and then crushed using a mortar and pestle. All

hydrogels were washed in approximately 325 mL of DI water for 24 hours and the dried, crushed particles were sieved between 75 and 250  $\mu\text{m}$ .

For dynamic mechanical analysis (DMA) 500  $\mu\text{L}$  of monomer solution, immediately following initiation, was added to a well of a 24-well cell culture plate and allowed to polymerize overnight.

### **2.2.3 Characterization**

3 mL of ovine plasma (3.8 % (w/v) acid citrate dextrose) were added to a vial containing 100 mg of dried hydrogel (1.5 M APM, 1.5 M acrylamide, 0.3 M BIS). The vial was then rotated for 18 hours on a Barnstead International (Dubuque, IA) Labquake.

For hematoxylin & eosin (H&E) staining sample slides were exposed to each stain for 90 seconds. For immunohistochemical (IHC) staining slides were incubated with a primary fibrinogen antibody (200  $\mu\text{L}$ , 62.5  $\mu\text{g}/\text{mL}$ ) for 60 minutes, followed by incubation with an Alexa Fluor 488-labeled donkey anti-goat IgG antibody (200  $\mu\text{L}$ , 5  $\mu\text{g}/\text{mL}$ ) for 60 minutes. Micrographs were taken with a Zeiss, Hitech Instruments (Broomall, PA), Axiovert 40 CFL microscope, and Diagnostic Instruments (Sterling Heights, MI) digital camera with corresponding software. For environmental scanning electron microscopy (ESEM) the coagulate complex was imaged using a FEI (Hillsboro, OR) Quanta environmental scanning electron microscope.

#### **2.2.4 Dynamic FVII Activation Experiment**

A set of 6 acrylamide-co-APM-co-BIS hydrogel compositions was tested in this experiment. The total concentration of APM and acrylamide was kept constant at 3 M, and only the comonomer ratio (acrylamide:APM:BIS) was varied. The HEM control (HEM CTRL) was composed of 1.5 M of HEM, 1.5 M of acrylamide and 0.3 M of BIS. The acrylamide control (Acrylamide CTRL) was composed of 3 M acrylamide and 0.3 M of BIS. 3.5 mL of human plasma (4 % (w/v) sodium citrate) were added to each vial containing 100 mg of dried, sieved hydrogel which was immediately rotated on a Labquake. 250  $\mu$ L aliquot plasma samples were taken at 30, 90, and 180 minutes. All aliquoted samples were filtered with Whatman (Piscataway, N.J.) .22  $\mu$ m Puradisc polyethersulfone membrane filters. The aliquoted samples were analyzed to determine FVIIa concentration using an American Diagnostica (Stamford, CT) *IMUBIND Factor VIIa ELISA*.

#### **2.2.5 Surface Area Dependence of FVII Activation**

Composition C (1.5 M APM, 1.5 acrylamide, 0.3 BIS) used in the above Dynamic FVII Activation Experiment was used to investigate the surface area dependence of FVII activation. Composition C along with the HEM CTRL (1.5 M HEM, 1.5 acrylamide, 0.3 M BIS) were synthesized according to the above protocol, washed for 24 hours in DI water, dried in a vacuum oven, and crushed using a mortar and pestle. The crushed particles were sieved to 4 different ranges; 53-150, 150-250, 250-355, and 355-425  $\mu$ m. 3.5 mL of human plasma (4 % (w/v) sodium citrate) were added to each vial containing 100 mg of dried, sieved hydrogel which was immediately rotated

on a Labquake. 250  $\mu$ L aliquot plasma samples were taken at 30, 90, and 180 minutes. All aliquoted samples were filtered with Whatman (Piscataway, N.J.) 0.22  $\mu$ m Puradisc polyethersulfone membrane filters. The aliquoted samples were analyzed to determine FVIIa concentration using an American Diagnostica (Stamford, CT) *IMUBIND Factor VIIa ELISA*.

### **2.2.6 Optimization**

156 different polymer hydrogels, varying in monomer composition, were prepared for the optimization experiment. 1.11 mL of human plasma (4 % (w/v) sodium citrate) were added to each vial containing 35 mg of dried hydrogel. The vial was then rotated for 18 hours on a Barnstead International Labquake. After the 18 hour cycle the coagulate complex was drained of plasma, and visually scored for fibrin formation on a scale of 0 (no fibrin formation) to 10 (substantial fibrin formation).

### **2.2.7 Dynamic Mechanical Analysis**

All hydrogel compositions tested in the Dynamic FVII Activation Experiment above were tested with a TA Instruments (New Castle, DE) Q800 dynamic mechanical analyzer under submersion compression mode. Hydrogel disks were immersed in DI water (multi-frequency) or citrated (4 % (w/v) sodium citrate), human plasma (stress-strain) for at least 18 hours. All samples were submerged in 1.5 mL of either DI water (multi-frequency) or human plasma (stress-strain) during

testing. Moduli were determined by fitting linear curves in the selected regions of strain.

### **2.2.8 Factor Deficient and Factor Inhibition Experiment**

The hydrogel composition of 1.5 M APM, 1.5 M acrylamide, and 0.3 M acrylamide (Composition C in above Dynamic FVII Activation Experiment) was tested with various factor deficient and factor inhibited plasmas. After the 18 hour cycle the coagulate complex was drained of plasma, and visually scored for fibrin formation on a scale of 0 (no fibrin formation) to 10 (substantial fibrin formation).

Factor deficient plasmas were prepared via the immunodepletion of citrated (4 % sodium citrated), normal human plasma (Haemtech Inc.). Factor inhibited plasmas were prepared by adding the necessary amount of chemical inhibitor to normal, human plasma (4 % (w/v) sodium citrate) to obtain the appropriate concentration for factor inhibition. CTI at a concentration of 7  $\mu\text{M}$  was used to inhibit FXIIa<sup>85</sup>. GGACK at a concentration of 500  $\mu\text{M}$  was used to inhibit FXa and PPACK at a concentration of 200  $\mu\text{M}$  was used to inhibit FIIa<sup>86</sup>. Although PPACK and GGACK have been shown to have secondary targets, their primary targets are FIIa and FXa respectively. 1.11 mL of factor deficient or factor inhibited human plasma were added to a vial containing 35 mg of dried hydrogel, which was then rotated for 18 hours. All rotations occurred on a Barnstead International Labquake.

### **2.2.9 TFPI Activity Experiment**

The same protocol used for the Dynamic FVII Activation Experiment including the same control compositions was used for the TFPI Activity Experiment. The aliquoted samples were then analyzed to determine TFPI activity using an American Diagnostica *ACTICHROME TFPI Activity Assay*. The *ACTICHROME TFPI Activity Assay* is a three stage chromogenic assay which measures active TFPI in plasma using a highly specific FXa substrate.

### **2.2.10 Artificial Plasma Experiment**

Composition C (1.5 M APM, 1.5 M acrylamide, 0.3 M BIS) along with the HEM CTRL (1.5 M HEM, 1.5 acrylamide, 0.3 M BIS), used in previous experiments were tested in this experiment. The artificial plasma was based on a platelet-suspension buffer used by Motlagh et. al.<sup>87</sup>, composed of 137 mM NaCl, 2.7 mM KCl, 0.4 mM sodium phosphate monobasic, 5.5 mM dextrose, 10 mM HEPES, 0.5 µg/mL FVII<sup>88</sup>, 10 µg/mL FX<sup>89</sup>, 100 µg/mL FII<sup>90</sup>, 7 µg/mL FV<sup>91</sup>, 5 µg/mL FIX<sup>92</sup>, 2.6 mg/mL FI<sup>89</sup>, and 30 µg/mL FXIII<sup>93</sup>. 1 mL of this artificial plasma was added to each vial containing 35 mg of dried hydrogel, which was then rotated for 18 hours. The resulting coagulate complex was stained for fibrin using the IHC protocol described above.

## 2.3 Results

We utilized a primary amine containing functional monomer, within various polymer hydrogel compositions, to help isolate the specific effects that positive electrostatic charge and mechanical microstructure have on FVII activation in citrated plasma. Histological and microscopic characterization techniques were used to investigate the formed coagulate complex. A dynamic FVII activation experiment confirmed the ability of multicomponent charged hydrogel compositions to induce FVII activation and offered insight into the dependence on electrostatic charge and mechanical structure. Dynamic mechanical analysis (DMA) was used to establish a correlation between polymer microstructure, and ability of the polymer hydrogel to induce FVII activation. Experiments utilizing artificial plasma, coagulation factor depleted and coagulation factor inhibited plasmas, and an assay capable of determining TFPI activity were conducted in order to elucidate the biological mechanism by which the charged material was inducing fibrin formation.

Due to the lack of free calcium in citrated plasma the kinetics of fibrin formation were considerably delayed, and because of this a longer incubation time (18 hours) was chosen for all experiments. This time period allowed for the qualitative assessment of the ability of the material to activate the cascade, based on the amount of fibrin formed. It should be noted that no fibrinolysis was observed in any of the experiments and that the formed clots were stable for several days after the 18 hour incubation period. An example of the clot formed by the hydrogel in the 18 hour cycle is shown in Figure 2.1.

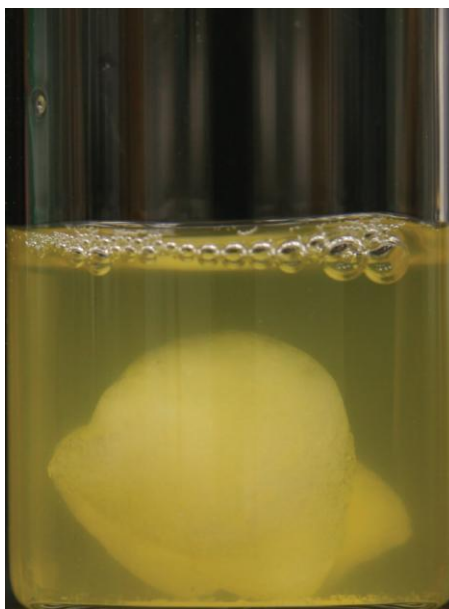


**Figure 2.1:** Typical coagulate complex (fibrin-hydrogel complex) formed after rotating a specific hydrogel composition (1.5 M APM, 1.5 M acrylamide, 0.3 M BIS) in human plasma (4 % (w/v) sodium citrate) for 18 hours. 300 mg of dried hydrogel were placed in 9 mL of plasma.

### 2.3.1 Characterization

Various histological and microscopic techniques were used to investigate the microstructure of the clot formed in the presence of the charged hydrogel (Figure 2.1). Initial IHC staining, using a primary fibrinogen antibody, was completed on the complex to confirm the presence of fibrin (Figure 2.2A). The fluorescence within the image clearly indicates the presence of fibrin within the complex, and suggests that the polymer is indeed activating the coagulation cascade. H&E staining was completed to confirm the acellular fibrous nature of the clot and also to investigate the physical interaction and geometric configuration of the polymer relative to the fibrin. The H&E stained micrograph, Figure 2.2B, clearly shows the presence of two distinct materials. The polymer hydrogel appears as the smooth, lighter colored material on the right side of the micrograph surrounded by a second fibrous material,

located on the left side of the micrograph. The darker, acellular, fibrous appearance of this material is consistent with fibrin staining.

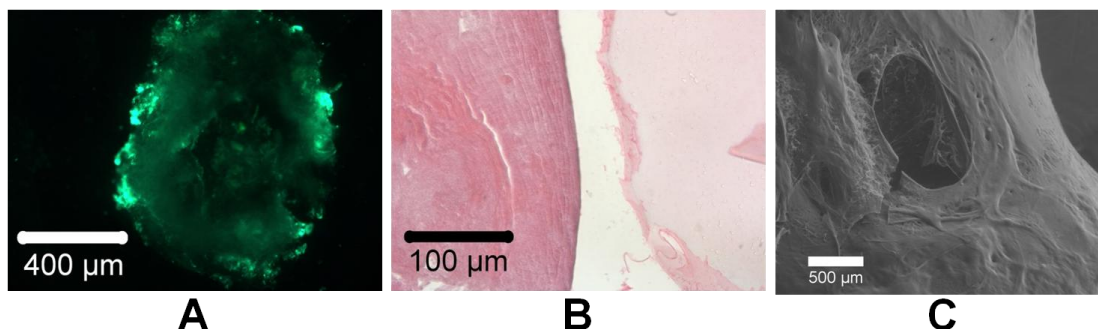


**Figure 2.2:** (A) IHC stained micrograph image of coagulate complex. (B) H&E stained micrograph image of coagulate complex. Polymer hydrogel appears as lighter, smoother material on right side of the micrograph while fibrin appears as the darker, rougher material on the left side of them micrograph. (C) ESEM surface image of the coagulate complex.

ESEM was completed in order to further investigate the characteristics of the complex. The ESEM image of the surface shows the presence of a continuous fibrin layer coating the exterior of the complex (Figure 2.2C). Cross-sectional images showed little to no fibrin presence within the interior of the complex suggesting initial generation of fibrin is occurring at hydrogel particle surface, eventually leading to the aggregation and envelopment of the particles resulting in a fibrin-covered composite.

### 2.3.2 Dynamic FVII Activation Experiment

Initial experiments in citrated plasma, depleted calcium environment, proved the ability of a positively charged material to induce the activation of the coagulation cascade resulting in the formation of a fibrin-based clot. A dynamic FVII activation experiment was completed in order to confirm the ability of such charged polymer materials to induce FVII along with investigate the critical material parameters

necessary for this activation. As Figure 2.3 shows, all compositions capable of inducing fibrin formation (compositions B, C, E) showed elevated levels of FVIIa compared to the controls (Figure 2.3, bar graph). All compositions incapable of inducing fibrin formation (compositions A, D, F) showed FVIIa levels similar to the controls, consistent with normal physiologic concentrations (~ 5 ng/mL). The elevated levels of FVIIa also closely correlated with the amount of fibrin formation generated by each respective composition (Figure 2.3, line graph). Composition C induces substantial activation of FVII resulting in FVIIa concentrations 8 times the resting levels (5 ng/mL) after 30 minutes and almost 15 times the resting concentration after 180 minutes.

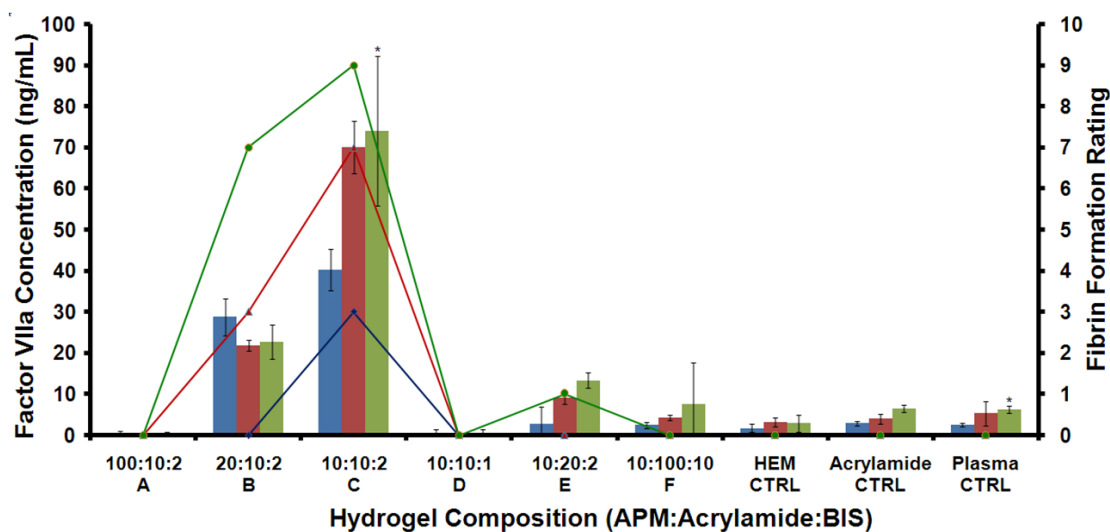


**Figure 2.3:** Factor VIIa concentration was measured in citrated human plasma containing various hydrogel compositions at 30, 90, and 180 minutes (left axis: bar graph). The amount of fibrin formation was also rated for each composition at each time point (right axis: line graph). Data is representative of an average and corresponding standard deviation (error bar) of three ( $n = 3$ ) separate sample trials. Asterisk (\*) indicates duplicate sample point.

The data also provides insight into the critical parameters of this activation suggesting that both electrostatic positive charge, e.g. primary amine functionality on the APM monomer, and polymer rigidity, i.e. cross-link density, are both crucial for

the activation of FVII. Composition A, which contains a high amount of APM concentration yet low amount of cross-linking monomer, BIS, is unable to induce FVII activation. Similarly, composition F which is highly cross-linked yet contains a minimal amount of positive electrostatic functionality, APM monomer, is also unable to induce FVII activation. Subsequent investigation was completed in order to develop a better understanding of the critical electrostatic and mechanical parameters necessary for FVII activation and subsequent fibrin formation.

### **2.3.3 Surface Area Dependence**

Previous experiments confirmed the ability of a positively charged polymeric hydrogel to induce the activation of FVII in citrated, platelet poor plasma. Further experimentation was conducted in order to determine if FVIIa generation could be correlated to surface area. The composition which was capable of inducing the optimum amount of FVIIa as shown in the previous Dynamic FVII Activation Experiment, composition C (1.5 M APM, 1.5 M acrylamide, 0.3 M BIS), was ground into 4 different particle sizes ranging from 53-425  $\mu\text{m}$  to determine if there was a correlation between FVII generation and surface area. A hydrogel composed of HEM (1.5 M HEM, 1.5 M acrylamide, 0.3 M BIS), used in the Dynamic FVII Activation Experiment, was used as a negative control. As Figure 2.4 below shows, there appears to be no correlation between the presented surface area of the hydrogel and FVIIa generation. The particles within the range of 53-150  $\mu\text{m}$  have considerably more surface area than the particles in the range of 355-425  $\mu\text{m}$  yet the difference in FVIIa generation is negligible indicating that particle surface area is a non-critical

parameter, at least between 50 and 450  $\mu\text{m}$ . The data suggests that the surface area exposed by 450  $\mu\text{m}$  particles is already sufficient to induce the activation of FVII, and increasing this surface area has no effect on enhancing the ability of the material to induce the phenomenon.

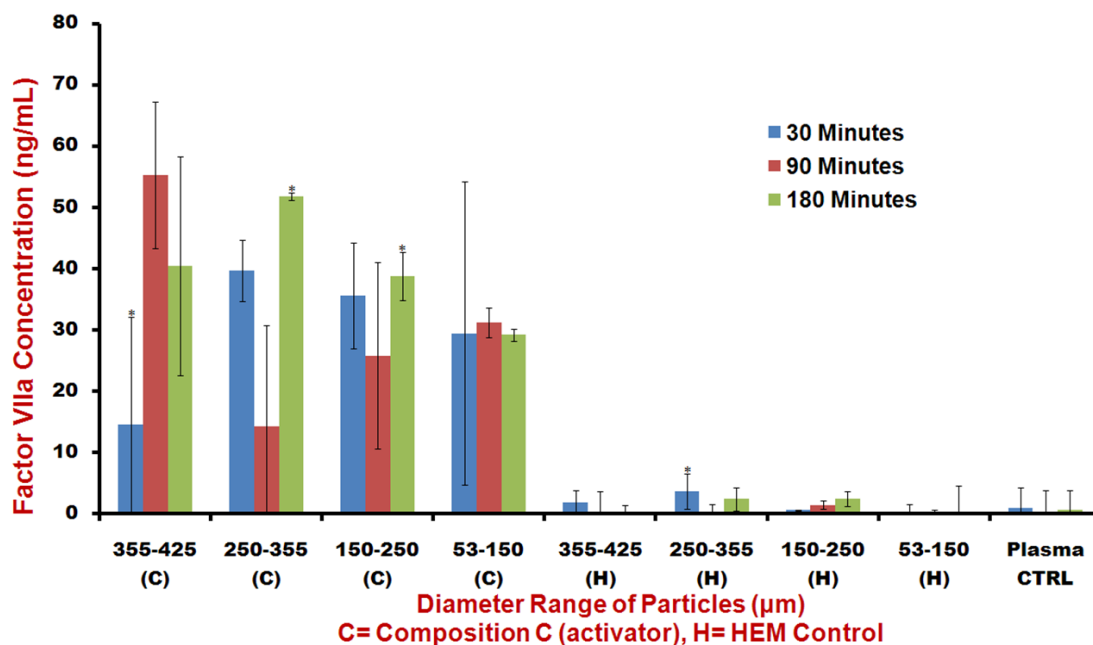


**Figure 2.4:** Factor VIIa concentration was measured in human plasma containing various particle sizes of a hydrogel capable of inducing FVII (composition C from above Dynamic FVII Activation Experiment) or a negative control (HEM Control) at 30, 90, and 180 minutes. Data is representative of an average and corresponding standard deviation (error bar) of three ( $n = 3$ ) separate sample trials. Asterisk (\*) indicates duplicate sample point.

### 2.3.4 Optimization

After a FVII activation experiment confirmed the ability of the polymer to induce the activation of FVII resulting in the subsequent formation of fibrin, an optimization study was conducted to investigate the effects that certain material and chemical properties had on the ability of the hydrogel to induce fibrin formation (FVII activation). Various compositions of polymer hydrogels were synthesized and tested with citrated, human plasma in order to determine the effects that monomer

concentration (APM + acrylamide + BIS), positive electrostatic charge (APM), and cross-linker ratio (acrylamide:APM:BIS) had on this phenomenon.

The data from this optimization experiment is arranged in a two dimensional grid, where each box depicts a specific monomer composition (Figure 2.5). The ability of each composition to induce fibrin formation was visually scored according to fibrin presence, from 0 (no fibrin formation) to 10 (substantial fibrin formation). Each composition box is color coded according to the rating scale located on the bottom of the figure. Images representative of fibrin formation ratings 0, 2, 4, 6, 8, and 10 are shown immediately below the scale for visual reference.

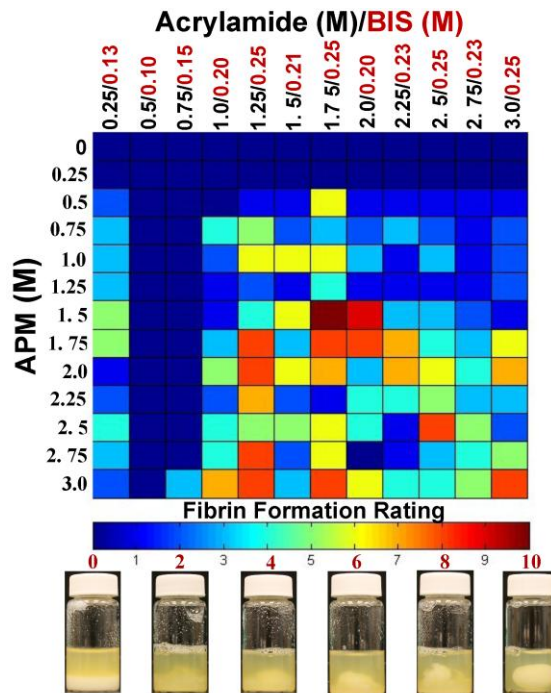


**Figure 2.5:** Experiment aimed to investigate the effect that various compositional factors including total monomer concentration (acrylamide + APM + BIS), positive electrostatic charge (APM), and cross-linker ratio (acrylamide:APM:BIS) had on fibrin formation (FVII activation). Acrylamide concentration is located on the horizontal axis while APM concentration is on the vertical axis. BIS concentration is also indicated on the horizontal axis and is kept constant for each respective acrylamide concentration. The amount of fibrin formation induced by each composition was visually scored from 0 (no fibrin formation) to 10 (substantial fibrin formation). Images of representative fibrin formation (clot) ratings 0, 2, 4, 6, 8, and 10 are displayed underneath the rating scale for visual reference. All samples were run in triplicate (n = 3).

No hydrogels composed purely of acrylamide and BIS were able to induce fibrin formation, indicating that the charge of the APM monomer, i.e. positive electrostatic charge on the primary amine, is vital to the process. It is also apparent from the data that the ability of the material to induce fibrin formation is highly dependent on the creation of a tightly cross-linked network. The 1.5 M APM concentration line (horizontal left to right) clearly indicates this dependence. At low acrylamide and BIS concentrations, the synthesized 3-component hydrogel is unable to induce fibrin formation, but as both of these parameters are increased, the ability of the hydrogel to induce fibrin increases considerably. This structural dependence is also evident, considering the composition capable of eliciting the optimum amount of fibrin shown in previous experiments (Composition C from Dynamic FVII Activation Experiment). This hydrogel consists of 1.5 M acrylamide, 1.5 M APM, and 0.3 M BIS. This optimum composition is able to induce a substantial amount fibrin, yet when the concentration of BIS is reduced from 0.3 to 0.15 M, the ability of the hydrogel to induce fibrin formation is completely lost. Increasing acrylamide and BIS concentration results in the creation of a more tightly cross-linked network, this in turn, leads to an increase in mechanical stiffness of the material. Results from this experiment suggest the appropriate balance of positive electrostatic charge and mechanical stiffness is essential to optimizing the polymer's ability to induce fibrin formation via the activation of FVII.

### 2.3.5 Dynamic Mechanical Analysis

The optimization experiment indicated that the ability of a polymeric hydrogel to induce FVII activation and subsequent fibrin formation in citrated plasma was dependent on both an electrostatic and mechanical component. Although several research groups have investigated the role of positive electrostatic charge in FVII activation in various medium, no groups, to the best of the authors' knowledge, have investigated the structural dependence of this activation in citrated (calcium depleted) plasma. Dynamic mechanical analysis (DMA) was used to investigate the relationship between specific mechanical properties and the ability to activate FVII and induce fibrin formation. DMA measures the mechanical properties of a material as a function of time, temperature, and frequency. There is a direct correlation of measured mechanical properties to microstructure. Multi-frequency experiments were conducted in order to investigate the heterogeneity of the material, while stress-strain experiments were conducted to determine stiffness and bulk mechanical properties.

The storage modulus is related to the stiffness of the material, while the loss modulus to damping and energy dissipation. Low frequency transitions are attributed to liquid-like properties of the material, where flow dominates. High frequency transitions are characteristic of more solid-like behavior, where elastic properties are prevalent. The multiple peaks in each composition's loss modulus clearly indicate that each polymer hydrogel is not homogeneous, but consists of multiple regions of mechanical equivalence. The compositions containing high to medium APM content (compositions A and C) show a transition at a lower frequency around 8 Hz,

indicating that these hydrogels contain a softer, more liquid-like region (Figure 2.6). The transitions of the low APM, high acrylamide composition (composition F) occur only in the higher frequency ranges, consistent with a stiffer material.

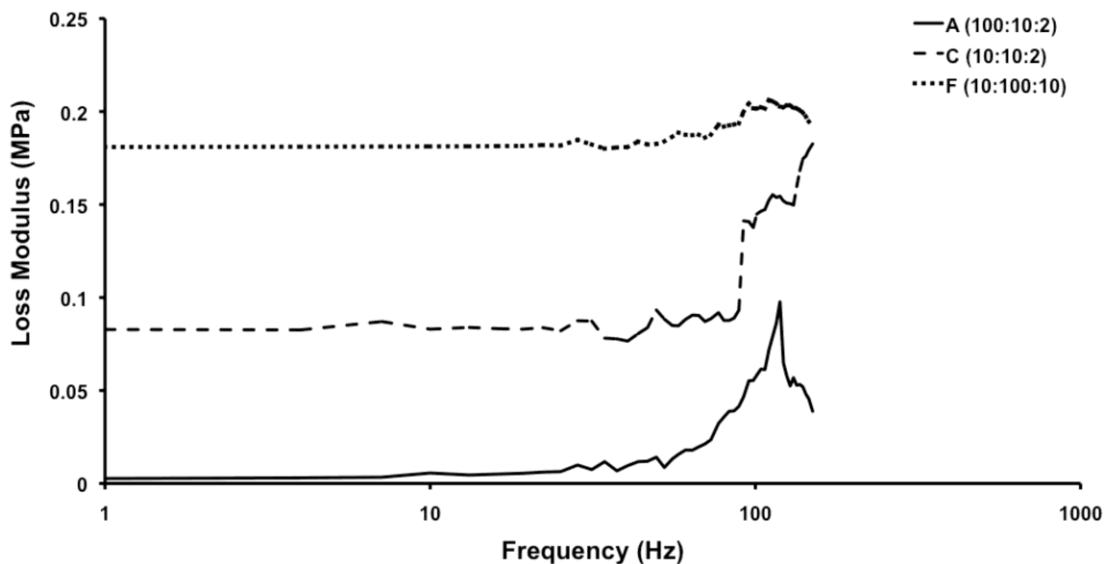


**Figure 2.6:** Graph of loss modulus vs. frequency of three compositions used in the Dynamic FVII Activation Experiment ranging from high APM, low acrylamide and BIS content (composition A) to low APM, high acrylamide and BIS content (composition F). Spectra for sample compositions C and F are shifted vertically to avoid overlapping of data. Spectra are representative of data obtained from several samples ( $n = 3 - 5$ ).

Stress-strain experiments were conducted to further corroborate a direct relationship between the mechanical stiffness of the hydrogel and its ability to induce FVII activation, and subsequent fibrin formation. As Figure 2.7 below shows, each composition exhibits distinctly different stress-strain behavior. Moduli for both the linear elastic region, between 0 % and 1 % strain, and the strain hardening region, between 4 % and 5 %, were determined to establish a quantitative assessment of material stiffness (Table 2.1). The moduli were calculated by fitting a linear regression to the data for each respective region and obtaining the slope. Of all the experimental samples, disregarding control samples, the optimum composition (composition C) has the largest linear elastic modulus along with the largest strain

hardening modulus. This enhanced stiffness of the optimum composition, most likely due to an ideal combination between physical and chemical cross-linking, along with the integration of positive charge results in a material capable of sustained activation of FVII and the corresponding coagulation cascade.

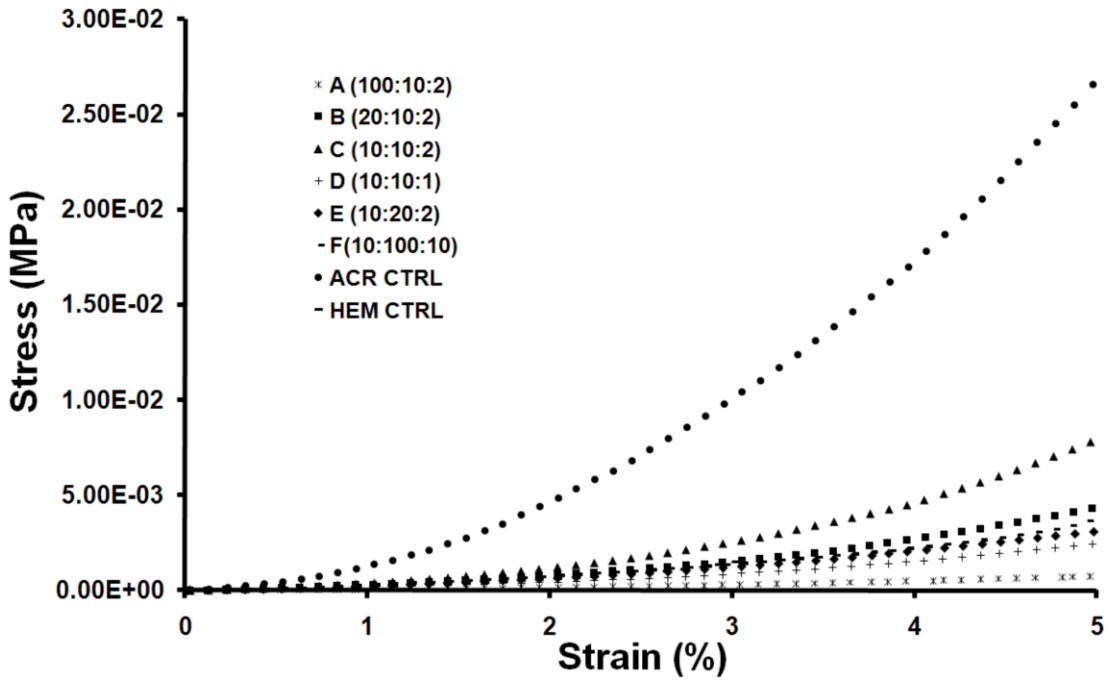


**Figure 2.7:** Stress-strain graph of all sample compositions used in the Dynamic FVII Activation Experiment. Curves are representative of data obtained from several samples ( $n = 3 - 5$ ).

Sample (APM:Acrylamide:BIS)	Modulus (Pa) (0 – 1 % strain)	Modulus (Pa) (4 – 5 % strain)
A (100:10:2)	90 ± 17	433 ± 153
B (20:10:2)	300 ± 71	1540 ± 358
C (10:10:2)	320 ± 45	2760 ± 439
D (10:10:1)	200 ± 100	900 ± 400
E (10:20:2)	160 ± 69	1000 ± 100
F (10:100:10)	200 ± 82	2000 ± 638
ACR CTRL	1225 ± 359	10500 ± 622
HEM CTRL	160 ± 55	N/A (sample yields)

**Table 2.1:** Both the linear elastic modulus (calculated between 0 % - 1 % strain) and the strain hardening modulus (calculated between 4 % - 5 % strain) were calculated for all sample compositions used in the Dynamic FVII Activation Experiment. The moduli were calculated by fitting a linear regression to the data for each respective region and obtaining the slope. 3 to 5 samples were used for each calculation (n = 3 – 5).

The relationship between material stiffness of the hydrogel and its ability to induce FVII activation and fibrin formation in citrated plasma is clearly demonstrated in the differences in elastic moduli between samples C and D. Both samples contain the identical amount of positive charge (APM) and differ only in cross-link density (BIS) yet, composition C is capable of strongly inducing FVII activation and fibrin formation, while composition D is incapable of inducing FVII activation and fibrin formation. This mechanical dependence is further corroborated by the stress-strain data from compositions A and C. Although, the amount of positive charge in composition A is almost twice that of composition C, composition A is incapable of inducing FVII activation and fibrin formation due to decreased material stiffness. This effect could also be attributed to a difference in charge density of the exposed surface as a result of water intake, or swelling, or the hydrogel. Future experiments

will be conducted in order to investigate the water uptake of specific polymer hydrogel compositions to determine if there is a correlation with FVII activation and fibrin formation. In any case, the results clearly demonstrate that there is a structural dependence on the ability of the polymer to induce FVII activation and fibrin formation. Furthermore, the results indicate that both electrostatic charge and adequate mechanical stiffness are necessary for the process and the appropriate balance of these two parameters leads to the creation of a polymer with optimized ability for FVII activation and fibrin formation.

### **2.3.6 Biological Mechanism**

Previous experimentation utilizing a FVIIa specific ELISA confirmed the ability of a polymeric hydrogel to induce the activation of FVII in citrated, platelet poor plasma. Furthermore, previous optimization experiments and dynamic mechanical analysis was used to help establish both an electrostatic and structural dependence for FVIIa activation within citrated plasma. Although these experiments helped to elucidate the critical material properties necessary for FVII activation they offered little insight into the biological mechanism by which fibrin formation was occurring. Successive experimentation was aimed at investigating the biological mechanism of tissue factor pathway activation and subsequent fibrin formation including the vital biological components and cofactors involved. Factor deficient and factor inhibited (chemical inhibition) plasmas were used to determine the biological factors which were vital to the mechanism. A specifically designed chromogenic assay was utilized to determine the effect that TFPI had in this activation. Finally an experiment using

artificial plasma was conducted in order to determine whether platelets, calcium, and TF were significant to the mechanism by which the polymer was inducing fibrin formation.

Experimentation utilizing various factor deficient and factor inhibited plasmas was completed in order to determine the coagulation factors which were vital to the mechanism by which the hydrogel was inducing fibrin formation (Figure 2.8).

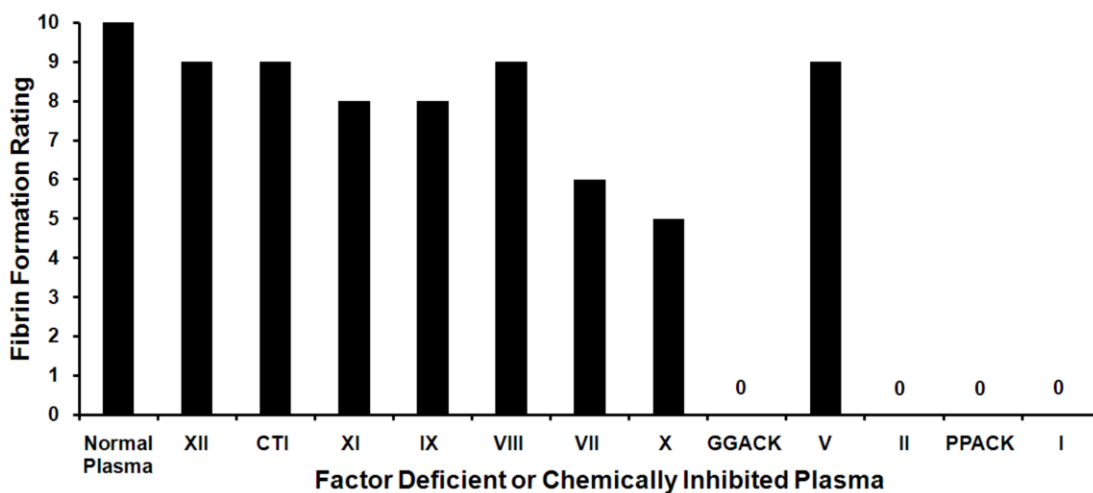


**Figure 2.8:** Optimum hydrogel composition (Composition C from above Dynamic FVII Activation Experiment) tested in various factor deficient and factor inhibited plasmas for 18 hours. After the 18 hour cycle the coagulate complex was drained of plasma, and visually scored for fibrin formation on a scale of 0 (no fibrin formation) to 10 (substantial fibrin formation). All samples were run in triplicate (n = 3).

As predicted by earlier experimentation, removal of FVII from plasma severely inhibited the ability of the hydrogel to induce fibrin formation relative to the normal, plasma control, indicating that FVII is indeed vital to the process. The small amount of fibrin formed is believed to be induced by the trace amounts of FVII not sufficiently removed in the purification process. Removal of FX also severely inhibited clotting. When FXa was inhibited using L-glutamyl-L-glycyl-L-arginine chloromethyl ketone (GGACK), complete inhibition of fibrin formation was

observed. These results, along with known mechanics of the coagulation cascade, suggest that FX is vital to the mechanism, and that the small amount of fibrin formed in the FX deficient plasma was induced by trace amounts FX not properly removed in the purification (immunodepletion) process. The removal of FII, or the chemical inhibition of FIIa using D-phenylalanyl-L-prolyl-L-arginine chloromethyl ketone (PPACK), led to complete inhibition of fibrin formation. Also, the data seems to agree with suggested theory of the ability of positively charged surfaces to initiate the autoactivation of FVII and further enhance or support the activation of FX and subsequently FII<sup>76,77,79-82</sup>.

Removal of FV, a cofactor of FII, had no significant effect on fibrin formation suggesting that this cofactor is not vital to fibrin formation in the presence of a positively charged surface at depleted calcium levels<sup>80,82</sup>. As predicted removal of FI, fibrin, resulted in complete inhibition of fibrin formation. Results from this experimentation suggest that FVII, FX, FII, and FI are all vital to the process, indicating that the biological mechanism of action of the polymer is via the activation of the tissue factor pathway, which leads to the subsequent activation of the common pathway, eventually resulting in fibrin formation.

Removal of FXII or chemical inhibition of FXIIa using corn trypsin inhibitor (CTI) showed little to no effect on fibrin formation when compared to normal human plasma. Similarly, removal of FXI had negligible effect on the ability of the polymer to induce fibrin formation, indicating that these factors, or rather the contact activation pathway, hold insignificant roles in the process.

Removing FIX from plasma did reduce fibrin formation but did not completely inhibit the process. While removal of FIX had a modest inhibitory effect on fibrin formation, removal of its primary cofactor FVIII had almost no effect on fibrin formation. While the data corroborates previous findings that positively charged surfaces are capable of enhancing the activation of FX by activated FIX in calcium depleted plasma, it further suggests that this mechanism is secondary to direct activation of FVII.

After investigating the vital coagulation factors and outlining a general mechanism of fibrin formation in the presence of charged hydrogels, experiments were conducted to understand roles that various cofactors and inhibitors had on this mechanism. Under normal physiologic circumstances, the FVIIa-TF-FX complex is rapidly bound and inhibited by TFPI. A strong electrostatic interaction could theoretically prevent TFPI from appropriately binding to its substrates, thereby reducing its inhibitory ability, although in the absence of TF, no TFPI activity is expected. To explore the role of TFPI in this process, a specifically designed TFPI activity assay (American Diagnostica *ACTICHROME TFPI Activity Assay*) was used. There appeared to be no outlying trend of TFPI activity for any of the experimental samples compared to the control samples (Figure 2.9), suggesting that the hydrogel is not interfering with the inhibitory activity of TFPI. The compositions which are able to induce fibrin formation (compositions B, C, E) showed no visible or statistical variation in TFPI activity compared to the rest of the experimental samples or any control samples. These results strongly indicate that the polymer is not interfering with the TFPI in the mechanism outlined.

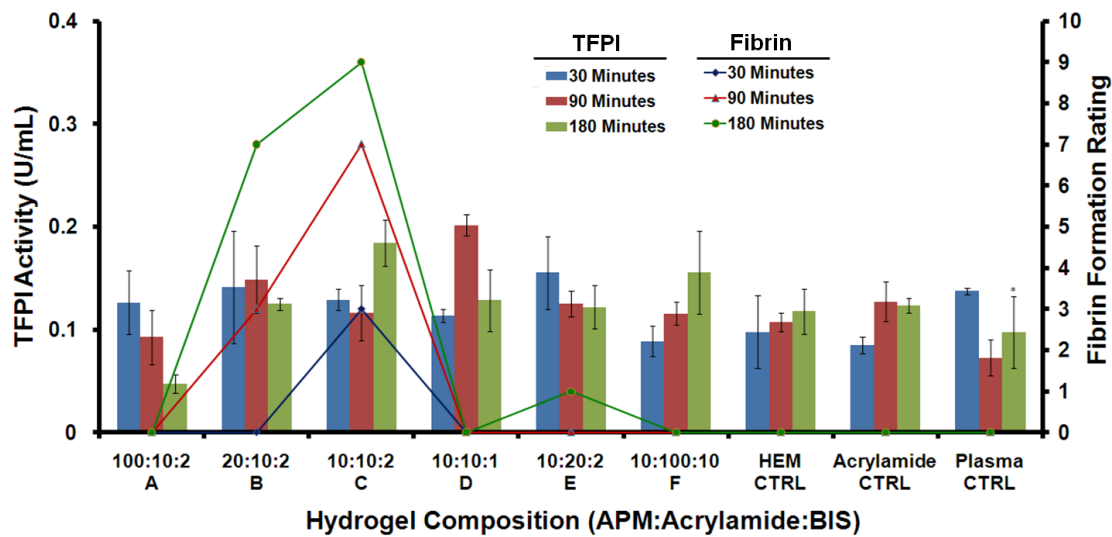


**Figure 2.9:** TFPI Activity was measured in human plasma containing various hydrogel compositions at 30, 90, and 180 minutes (left axis: bar graph). The amount of fibrin formation was also rated for each composition at each time point (right axis: line graph). Data is representative of an average and corresponding standard deviation (error bar) of three (n = 3) separate sample trials. Asterisk (\*) indicates duplicate sample point.

The complete and successful activation of the tissue factor pathway requires the coordination and interaction of a multitude of cofactors including calcium, platelets, and TF. Previous work by has shown the ability of positively charged polymers to induce the autoactivation of FVII and to assist in the activation of FX by FVIIa and FIXa in medium with depleted calcium levels. Although platelets and TF enhance this process it has been shown that these cofactors are not necessary for these activation steps. To further investigate the role of these cofactors in the biological mechanism, an experiment was conducted using “artificial plasma” consisting of only FVII, FIX, FX, FV, FII, FXIII, and FI (fibrin) and explicitly lacking calcium, TF, and platelets.

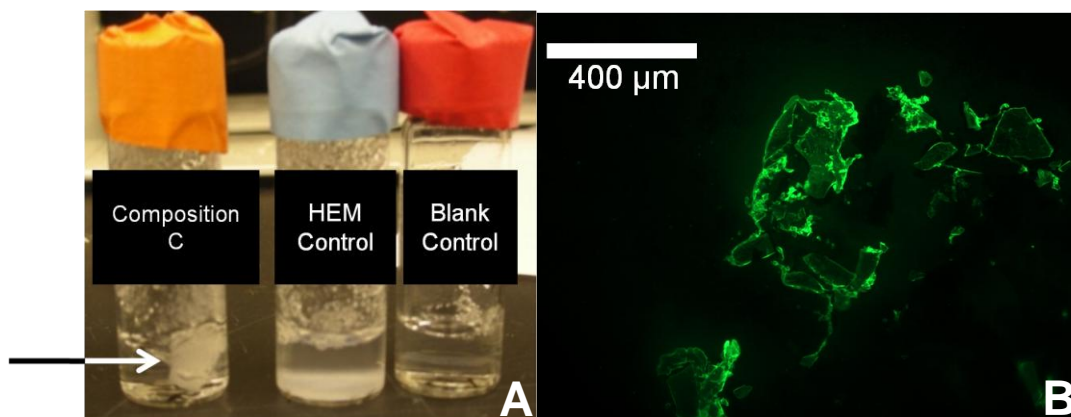


**Figure 2.10:** (A) Image of hydrogel capable of inducing optimum FVII activation, Composition C used in previous experimentation, (orange cap), along with a HEM control hydrogel (blue cap) and a blank control (red cap) after 30 minute rotation in artificial plasma explicitly lacking calcium, tissue factor (TF), and platelets. Arrow shows fibrin clot formation. Artificial plasma consisted of 137 nM NaCl, 2.7 mM KCl, 0.4 mM sodium phosphate monobasic, 5.5 mM dextrose, 10 mM HEPES, 0.5  $\mu\text{g}/\text{mL}$  FVII, 10  $\mu\text{g}/\text{mL}$  FX, 100  $\mu\text{g}/\text{mL}$  FII<sup>31</sup>, 7  $\mu\text{g}/\text{mL}$  FV<sup>32</sup>, 5  $\mu\text{g}/\text{mL}$  FIX, 2.6 mg/mL FI, and 30  $\mu\text{g}/\text{mL}$  FXIII. (B) IHC stained image of clot formation observed with composition C.

As Figure 2.10 shows the composition C was able to induce fibrin formation in the artificial plasma within minutes, and by 30 minutes a substantial fibrin-based aggregate formed which was confirmed using IHC. Although the artificial plasma was also void of the inhibitory mechanisms naturally present in plasma, the results do indicate that the polymer is capable of inducing fibrin formation through the rapid activation of FVII independent of calcium, platelets, and TF.

## 2.4 Discussion

Charged polymer hydrogels were used to help elucidate a better understanding of the critical material properties necessary for the activation of FVII and subsequent fibrin formation in citrated, platelet-poor plasma. Characterization experiments confirmed the generation of fibrin and also provided insight into the microstructure of clot formation. A FVII ELISA was used to confirm the ability of various charged

polymer hydrogels to induce FVII activation. The results of the Dynamic FVII Activation Experiment suggested that cross-link density or mechanical rigidity, in addition to positive electrostatic charge, was crucial to FVII activation. Dynamic mechanical analysis was conducted in order to establish a structural correlation between the mechanics of the polymer microstructure and FVII activation. Experiments utilizing factor deficient and factor inhibited plasmas showed that FVII, FX, FII, and FI are all vital to the process, outlining the general mechanism of coagulation activation and fibrin formation. A TFPI activity assay indicated that the inhibitor had little effect on the ability of the charged polymer to induce FVII activation and fibrin formation, most likely due to the lack of TF in the media.

Several of the protein factors which play a vital role in the ability of the material to induce fibrin formation, i.e. FVII, FX, and FII, are vitamin-K dependent serine proteases. Previous research has found that these proteins may be separated from various other coagulation proteins through the presentation of a highly positively charged surface and furthermore that such positively charged surfaces are capable of enhancing the activation of these coagulation factors in calcium depleted media<sup>76-82,94</sup>. It is believed that the coordination of these factors occurs through the electrostatic binding between the positively charged surface and the Gla domains of the enzymes. In calcium depleted medium the majority of the Gla domains of these factors lack calcium which results in the presentation of a highly negatively charged capable of interacting with a positively charged surface<sup>76-82,94</sup>. Although the role of electrostatic charge in this phenomenon is well known we have shown that there is also a critical structural parameter. Dynamic mechanical analysis elucidated that there is a clear

correlation between the rigidity of the material, i.e. elastic and strain hardening modulus, and the ability of the material to induce FVII activation resulting in fibrin formation. Previous reports have suggested that the molecular weight and/or the concentration of polymer used are the key parameters yet our results indicate that it is the structural rigidity of the charged surface which determines the ability of the polymer to induce FVII activation.

A better understanding of the interactions that occur between synthetic surfaces and biological substrates is key to the development of future biomaterial technology. It is imperative we understand the critical parameters which are able to affect in vivo biological processes, specifically the coagulation cascade, in order to develop more effective and safer blood-contacting biomaterials.

## **3 Chapter 3: Clinical Diagnostic and Animal Experimentation**

### **3.1 Introduction**

The body's initial response to injury involves the selective deposition and adherence of platelets to the subendothelium layer of the disruption site via collagen. Interaction with collagen and other molecules contained within the subendothelium, e.g. ADP, also activates the platelets inducing the formation of several pseudopodia tentacles. Activation also induces platelets to release several molecules including fibrinogen, ADP, vWF, platelet factor 4, and thrombospondin, which assist in subsequent platelet aggregation and activation. Initial activation, aggregation, and deposition of platelets to the wound site is crucial to the formation of a platelet plug to control initial blood loss. This platelet plug is eventually stabilized by fibrin to produce a robust hemostatic clot.

Previous *in vitro* experimentation focused on investigating the specific material factors which affect the activation of the coagulation cascade in citrated plasma, specifically the activation of FVII. Subsequent research utilizing clinical diagnostic and live animal experiments was conducted in order to investigate the critical material parameters key to promoting the formation of an effective platelet plug in a clinically relevant model. The end goal of this research was the translation of *in vitro* and *in vivo* clinical diagnostic findings to develop an effective hemostatic material.

## 3.2 Materials and Methods

### 3.2.1 Materials

Acrylamide, N,N'-methylenebisacrylamide (BIS), N,N,N',N'-tetramethylethylenediamine (TEMED), and ammonium persulfate (APS) were purchased from Sigma-Aldrich (Milwaukee, WI). N-(3-aminopropyl)methacrylamide hydrochloride (APM) was purchased from Polysciences (Warrington, PA). N-(2-hydroxyethyl)methacrylamide (HEM) was purchased from Monomer-Polymer (Trevose, PA). Deionized water (DI water) was obtained using a Millipore Super-Q water system (Billerica, MA). Plastic capped glass vials were purchased from VWR Scientific (West Chester, PA).

### 3.2.2 Hydrogel Synthesis

A specific amount of either acrylamide, N,N'-methylenebisacrylamide (BIS), N-(2-hydroxyethyl)methacrylamide (HEM), or N-(3-aminopropyl)methacrylamide hydrochloride (APM) was dissolved in DI water and mixed thoroughly until all components were completely solvated. The solution was then titrated to a pH between 6.8 and 7.2 using sodium hydroxide (NaOH) and/or hydrochloric acid (HCl). After pH adjustment, the monomer solution was initiated by adding 20  $\mu\text{L}/\text{mL}$  of a 7.5 % (v/v) N,N,N',N'-tetramethylethylenediamine (TEMED) solution, followed by adding 20  $\mu\text{L}/\text{mL}$  of a 15 % (w/v) solution of ammonium persulfate (APS), for polymerization. For the fresh sheep blood experiments the hydrogels were crushed after formation and portioned accordingly for testing. For all animal clinical trials the hydrogels were washed in approximately 325 mL of DI water for at least 24 hours,

dried in a vacuum oven overnight, crushed with a mortar and pestle, and sieved to obtain particles between 75 and 250  $\mu\text{m}$ .

### **3.2.3 Sheep Blood Experiments**

Fresh blood was taken intravenously from an adult Dorsett hybrid sheep (~ 65 kg). After drawing approximately 1 mL of fresh blood was added to a glass or polypropylene vial, containing 250 mg of hydrogel sample. The ability of the hydrogel to form a clot was visually observed. During the course of the study, all animals received humane care in accordance with the Guide for Care and Use of Laboratory Animals (National Institutes of Health publication 86-23, revised 1996).

### **3.2.4 In Vivo Animal Experiments**

All surgeries were completed on an adult Dorsett hybrid sheep (~ 65 kg). Anesthesia was induced with thiopental sodium (10 mg/kg) and maintained by mechanical ventilation with 1 % - 2 % isoflurane mixed with oxygen. A Draeger anesthesia monitor (North American Draeger, Telford, Pa) was used during the surgery. Immediately after the surgery the respective tissue (lung or liver) was excised, and analyzed using various staining techniques including hematoxylin & eosin (H&E) and Carstairs' method. The surgical protocol and animal care were approved by the Institutional Animal Care and Use Committee of the University of Maryland, Baltimore.

#### **3.2.4.1 Lung**

An incision, approximately 5 cm in length and 1 cm in depth, was made with a surgical scalpel on the anterior or ventral side of the sheep's lung. The hydrogel bandage was then applied to the wound site, with slight pressure, for approximately 2 minutes. The bandage consisted of simple gauze with 1500 mg of dried hydrogel (2.73 M APM, .27 M acrylamide, .054 M BIS) on the surface. 5 mL of DI water were sprayed on the bandage to facilitate the adherence of the hydrogel to the gauze.

#### **3.2.4.2 Liver**

An incision, approximately 5 cm in length and 1 cm in depth, was made with a surgical scalpel on the anterior or ventral side of the sheep's liver. Approximately 750 mg of dried hydrogel were poured into the laceration, which was then compressed with gauze for approximately 4 – 5 minutes.

#### **3.2.4.3 Histological Staining**

5  $\mu\text{m}$  sections of each respective incision site (lung or liver) were obtained and set in paraffin. The sections were then deparaffinized with xylene and rehydrated with a series of graded alcohol solutions. Hematoxylin and eosin (H&E) along with the Carstairs' method of platelet staining was completed on the samples.

### **3.3 Results**

Initial in vitro experiments focused on understanding the material parameters which effect coagulation cascade activation and fibrin formation in citrated, platelet poor plasma. Subsequent research utilizing fresh blood and in vivo animal trials was conducted to understand the critical material components key to the formation of an effective hemostatic seal in vivo. The specific goal of the research was to determine the viability of a charged polymer hydrogel to effectively control blood loss in a clinically relevant model.

#### **3.3.1 Sheep Blood Experiments**

Experimentation utilizing unadulterated (lacking any type of anticoagulation) sheep blood drawn directly from the animal was conducted to identify and isolate the vital material properties associated with rapid and effective clot formation. Initial experiments in the presence of a FXII activation surface (glass surface) showed the ability of specific formulations to induce rapid platelet aggregation resulting in a robust hemostatic clot within 5 minutes. Polymeric hydrogels systemically ranging in both positive electrostatic charge and mechanical stiffness were synthesized and tested with sheep blood in the presence of a coagulation cascade activator (glass surface). Within the presence of a coagulation activator hydrogel compositions consisting of higher amounts of electrostatic charge (increased ratio of APM:acryamide + BIS) and lower cross-link density (decreased ratio of BIS:APM+acrylamide) were capable of eliciting the most rapid and effective clot

formation. A specific polymer formulation consisting of 2.73 M APM, 0.27 M acrylamide, and 0.054 M BIS was capable of inducing the formation of a robust clot within 3 minutes compared to a control which took over 10 minutes. Subsequent qualitative inspection of the clots showed that the clot formed by the hydrogel was considerably more robust than the control (Figure 3.1).

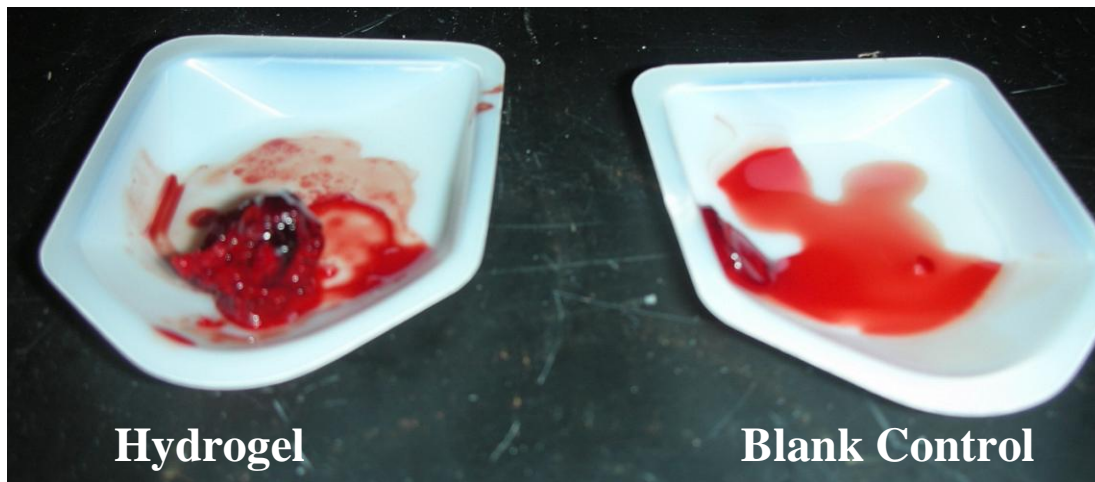


**Figure 3.1: Clot Formation in Sheep Blood.** Clot formations induced by the hydrogel compared to a blank control. Approximately 1 mL of sheep blood, drawn directly from the animal, was added to a glass vial containing 250 mg of polymer hydrogel (2.73 M APM, 0.27 M acrylamide, and 0.054 M BIS) along with a blank glass vial. Clot formation was induced by the hydrogel in approximately 3 minutes compared to clot formation observed in the blank control which took over 10 minutes.

Experiments were also conducted in polypropylene vials to investigate the ability of specific hydrogel formulations to induce clot formation without the addition of a coagulation cascade activator (glass surface). Without the addition of a coagulation activator, polymeric hydrogels consisting of higher electrostatic charge and lower cross-link density, lower mechanical stiffness, were incapable of inducing fibrin formation. Although these hydrogel formulations dramatically increased the viscosity of the blood, most likely due to the absorption of water, platelets, and erythrocytes, they delayed the onset of fibrin formation compared to a blank control sample. Contrary to hydrogels composed of higher amounts of electrostatic positive charge

and lower cross-link density, formulations of lower amounts of positive charge and higher cross-link density expedited the onset of fibrin formation. Furthermore, experimentation showed that a hydrogel composition which completely inhibited fibrin formation could be engineered to promote the onset of fibrin formation by increasing cross-link density, regardless of positive electrostatic charge.

The results of this blood experimentation clearly indicated the importance of both positive electrostatic charge and cross-link density in both primary and secondary hemostasis. Increased positive electrostatic charge and decreased cross-link density seemed to enhance the ability of the polymer to aggregate platelets and erythrocytes yet inhibited coagulation cascade activation. Hydrogels composed of lower amounts of positive electrostatic charge and higher cross-link density expedited fibrin formation yet were ineffective at forming a robust platelet plug do to, what is believed to be, the inability to absorb platelets and erythrocytes. Subsequent animal experimentation was conducted in order to further investigate the critical material properties involved with primary and secondary hemostasis in vivo.

### **3.3.2 In Vivo Animal Experiments**

Previous sheep blood experimentation had shown that hydrogel compositions consisting of higher positive electrostatic charge and lower cross-link density were better able to induce the aggregation of platelets and erythrocytes to generate an effective hemostatic plug, especially in the presence of an activator. In vivo animal experimentation was conducted in order to determine whether the obtained in vitro results could be translated to in vivo. The specific goal of this animal

experimentation was to investigate the ability of a charged polymer hydrogel to control hemorrhaging in a clinically relevant model. The global aim of the research sought to identify the key material properties which were vital to enhancing both primary and secondary hemostasis to induce the formation of an effective hemostatic clot.

All experimentation was conducted on adult hybrid Dorsett sheep. Sheep were chosen as a model due to the fact that their arteries are similar in size to that of humans, and their coagulation and fibrinolytic systems are closer to those of humans relative to that of a canine or swine<sup>95,96</sup>.

### **3.3.2.1 Lung**

Immediately after the incision was made a gauze pad containing the hydrogel was placed directly on the wound site, to which slight pressure was applied for 1 minute (Figure 3.2A-B). After 2 minutes the gauze pad containing the hydrogel was removed and the wound site was washed with saline solution and visually inspected. As Figure 3.2C shows the hydrogel was able to completely seal the incision effectively stopping blood loss in approximately 2 minutes. Immediately after the experiment, the lung was excised in order to conduct histological staining on the incision site.

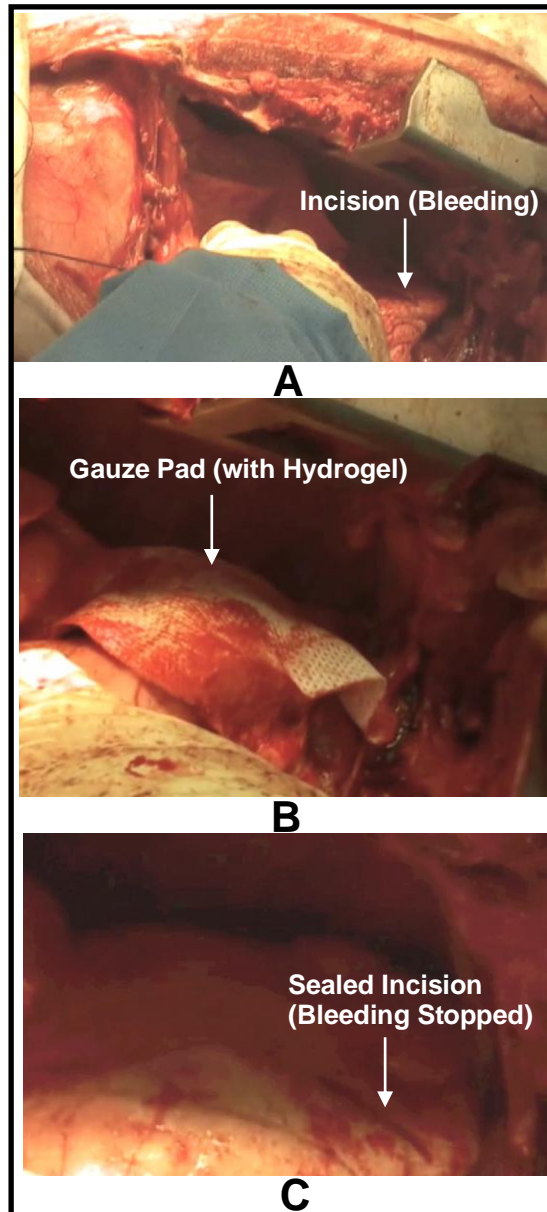


**Figure 3.2:** Image of lung incision site before hydrogel is applied (A), during the application of the hydrogel (B), and after the hydrogel is removed (C).

Hematoxylin & eosin staining was conducted on the incision site to investigate the microstructure of the clot (Figure 3.3). The stained micrographs show the presence of a fibrin matrix embedded with various types of cells including erythrocytes, leukocytes, and platelets consistent with the microstructure of a typical hemostatic platelet plug. The results from the histological staining confirmed the

ability of the hydrogel to induce the formation of an effective hemostatic platelet plug to control blood loss.

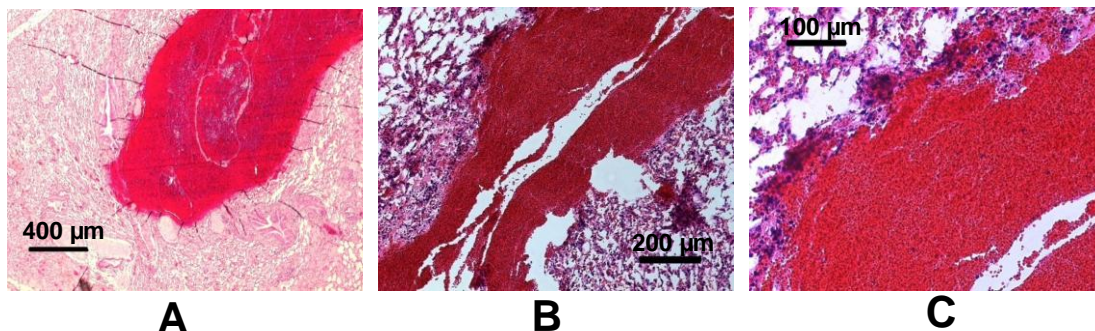


**Figure 3.3:** Optical micrographs of H&E stained sections of the lung incision site. Magnifications of 5x (A), 10x (B), and 20x (C).

### 3.3.2.2 Liver

After confirming the ability of the hydrogel to induce rapid and effective hemostasis on the lung, experiments were conducted on the liver to determine if the hydrogel could control more severe hemorrhaging. The liver is considerably more vascularized than the lung which makes hemorrhaging from the liver incredibly difficult to control. Simple compression is typically unable to stop blood loss from the liver and the delicacy of the tissue makes it very hard to suture with conventional stitches. A material capable of inducing rapid and effective hemostasis on the liver would be a great benefit to the field.

The protocol for the liver incisions was kept consistent with the protocol used for previous lung experimentation. Immediately after the incision was made the hydrogel was applied to the wound site where slight pressure was applied with a gauze pad for approximately 5 minutes. After 5 minutes the pad was removed and the wound site was washed with saline solution and visually inspected.

Several different hydrogel compositions were tested and, as in the case with the lung experiment, the composition consisting of 2.73 M APM, 0.27 M acrylamide, and 0.3 M BIS was able to induce hemostasis most effectively. The polymer was able to induce complete hemostasis in approximately 5 minutes. Figure 3.4B clearly shows that the hydrogel was able to induce a robust hemostatic seal, effectively stopping blood loss from the wound site.

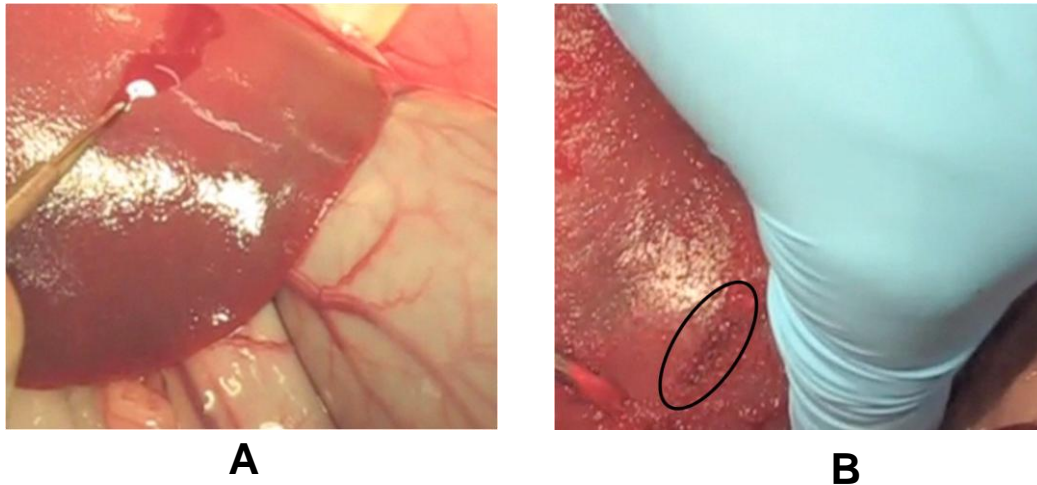


**Figure 3.4:** (A) Image of the initial liver incision site, before hydrogel is applied. (B) Image of same site after the hydrogel is removed. Complete hemostasis was observed in 5 minutes.

Histological staining of the wound site was completed immediately after the experiment in order to further investigate the microstructure of the hemostatic seal. H&E staining confirmed the formation of an effective hemostatic clot at the wound site (Figure 3.5). Substantial fibrin formation can be seen within the incision site, bridging the wound from each tissue. Much of the fibrin formation is emanating from the surfaces of the hydrogel particles suggesting that the particles provided an active surface for coagulation activation and subsequent fibrin generation. Furthermore, several cell-like bodies, which are believed to be erythrocytes, platelets, and/or

leukocytes, are embedded within the fibrin matrix forming what appears to be an effective hemostatic plug.

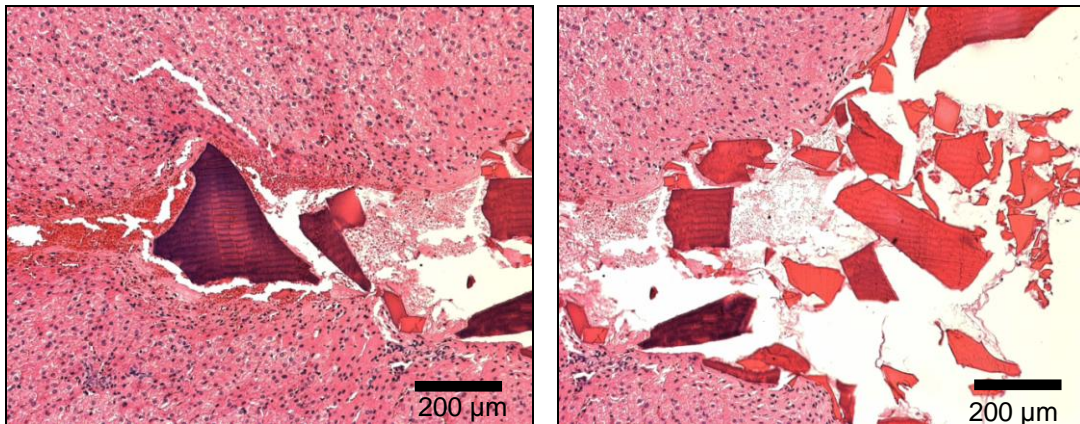


**Figure 3.5:** H&E stained micrographs of the liver incision site.

Carstairs' histological method was used to positively identify the critical components of the hemostatic seal (Figure 3.6). Carstairs' method is a common histological technique to distinguish platelets (grey), fibrin (orange-red), collagen (blue), platelets (grey), and erythrocytes (red-yellow).

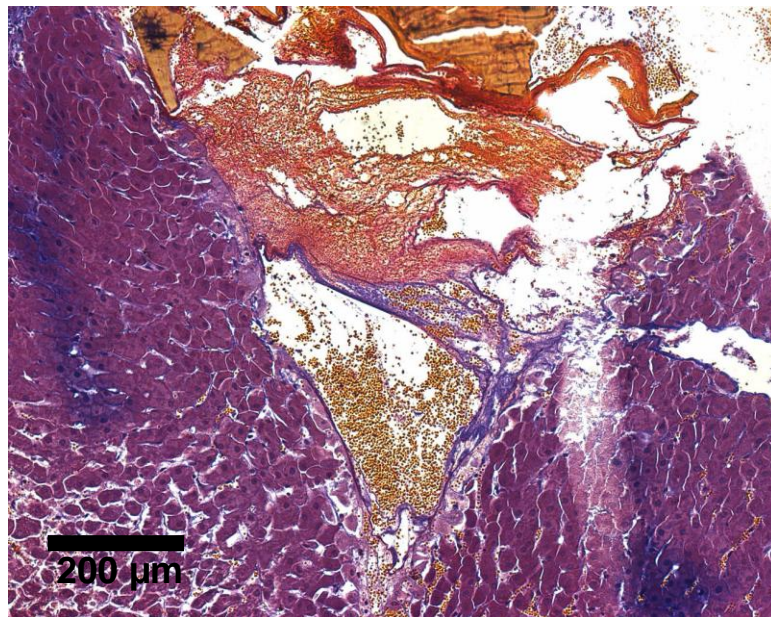


**Figure 3.6:** Carstairs' Method stained micrographs of liver incision site. Fibrin (red-orange), collagen (blue), erythrocytes (red-yellow), platelets (grey).

Carstairs' staining positively confirmed the generation of fibrin at the incision site. The micrographs agree with H&E stained images of the incision site indicating that fibrin generation spawns from the hydrogel particles into the wound. Platelets and erythrocytes (yellow and grey particles) can be observed both within the fibrin mesh along with deep inside the wound site. Results from the histological staining clearly demonstrated the ability of the hydrogel to induce and enhance the formation of a platelet plug which was capable of effectively controlling blood loss.

### **3.4 Discussion**

Experimentation using sheep blood suggested positive electrostatic charge and cross-link density were key determinants of the ability of the material to induce or enhance clot formation. Hydrogel formulations composed of higher amounts of positive electrostatic charge and lower cross-link density were able to effectively induce and enhance clot formation in the presence of a coagulation activator. Interestingly, without the addition of a coagulation cascade activator such hydrogels delayed and in some cases completely inhibited fibrin formation, which subsequently inhibited the formation of an effective clot. Hydrogel compositions of higher cross-link density enhanced the onset of fibrin formation yet were not nearly as effective at aggregating platelets and erythrocytes.

Both platelets and erythrocytes have a net negative charge, therefore increasing the positive electrostatic charge of the hydrogel should increase its affinity for both platelets and erythrocytes due to an increased electrostatic attraction. Decreasing

cross-link density allows the hydrogel to swell more, take up more liquid volume which most likely aids in both obstructing blood flow and adhering more platelets, erythrocytes, and leukocytes to generate a more effective platelet plug. On the other hand, it seems stiffness, i.e. cross-link density, is a key parameter in order to effectively enhance the activation of the coagulation cascade in fresh blood. Without the presence of an activator, hydrogels of lower cross-link density, lower stiffness, delayed the onset of fibrin formation and in some cases completely inhibited the process. Interestingly, regardless of electrostatic charge, the ability of a polymer hydrogel to enhance fibrin formation could be tuned by changing only the relative cross-link density ranging from complete inhibition (low cross-link density) to acceleration (high cross-link density) of the process. Results indicate that the structure or stiffness of the hydrogel is crucial to providing an effective surface for coagulation cascade activation.

In vivo experimentation confirmed that hydrogels containing higher electrostatic charge with low cross-link density are more effective at controlling blood loss. Highly cross-linked hydrogel formulations were ineffective at stopping blood loss, regardless of the amount of electrostatic charge. A specific hydrogel formulation consisting of 2.73 M APM, 0.27 M acrylamide, and 0.3 M BIS was able to induce complete hemostasis of a lung incision in 2 minutes. The same hydrogel was able to induce a hemostatic seal of a similar sized incision on the surface of the liver in approximately 5 minutes. Histological staining of the wound site clearly indicated that the hydrogel was able to induce the formation of an effective hemostatic plug, composed of platelets and erythrocytes, stabilized by fibrin.

Furthermore, the images indicated that fibrin formation generated from the hydrogel particles suggesting that coagulation cascade activation was occurring on or in close proximity to the hydrogel surface.

Biological-based hemostatics including those based on fibrin and/or thrombin typically take approximately 3 - 5 minutes to induce complete hemostasis of an internal organ incision such as the liver. The fact that the hydrogel tested was capable of inducing a robust seal in approximately 5 minutes attests to the viability of such a material to be used as a surgical hemostatic. Such a polymer-based hemostatic would have tremendous advantages over its biological counterparts including a lengthened shelf life, ease of production, no risk of virus transmission or biologically induced allergic reaction, and most importantly low price. Such a synthetic hydrogel could be produced at a fraction of the price of its biological counterparts making such a material a viable option for developing countries where 90 % of blood loss deaths occur. Research into the understanding of how synthetic materials interact with the body's clotting process is integral to developing a safe, inexpensive, and effective material capable of enhancing or assisting it. This research is key to the development of the next generation of hemostatic materials which will save millions of people around the world every year.

## **4 Chapter 4: Contributions and Future Work**

### **4.1 Contributions**

This work represents a thorough investigation into how both electrostatic charge and mechanical stiffness of a polymer hydrogel material affect FVII activation in citrated plasma. Combined with known biochemical mechanism of FVII auto activation in the presence of a charged surface, this work substantiates the contributing material properties which influence this activation.

The clinical research conducted clearly indicates that positive electrostatic charge and cross-link density, i.e. mechanical stiffness, are key factors in determining the ability of a polymer hydrogel to promote or enhance hemostasis. It was determined that although hydrogels containing higher positive electrostatic charge with low cross-density delayed or inhibited fibrin formation (blood coagulation activation) they were effective at enhancing and promoting platelet plug formation in the presence of an activator. On the other hand, although stiffer hydrogels, i.e. hydrogels containing higher cross-link densities, were capable of expediting the onset of coagulation activation and subsequent fibrin formation they were ineffective at inducing the formation of an effective hemostatic plug.

In vivo animal experimentation confirmed the ability a specific charged polymer hydrogel to induce hemostasis in a clinically relevant model. Furthermore, this experimentation indicated that positive electrostatic charge and cross-link density were key material parameters which affect the hemostasis in vivo. Histological staining of the incision sites revealed that the hemostatic seal induced was composed

of platelets and erythrocytes stabilized by fibrin generated from the surface of the particles.

This research has contributed to a better understanding of the activation mechanism of coagulation proteins, specifically FVII, which is crucial to the design of a system capable of safely and effectively enhancing this activation. From a clinical viewpoint this research provides a clear correlation between specific material properties of a synthetic polymer-based material and corresponding influence on the body's clotting response. Understanding how specific coagulation components interact with material chemistries is vital to the development of any engineered blood contacting materials including but not limited to artificial organ coatings, in vivo therapeutic delivery systems, and stents. In conclusion, it is the hope of the author that this research lays the foundation for the development of future biomaterials capable of influencing or manipulating blood-based physiological processes which will help millions of people in the future.

## **4.2 Future Work**

Future work will focus on developing a better understanding of the material properties which affect hemostasis in vivo. Experiments utilizing unadulterated, lacking anticoagulation, human and sheep blood will be conducted to determine the influences that specific material properties have on the activation of coagulation factors. Further clinical diagnostic experimentation, including platelet aggregometry and thromboelastography will be conducted in order to investigate the material

determinants involved with platelet activation, aggregation, and eventual plug formation.

In terms of material synthesis, efforts will be made to alter the chemistry of the synthesized polymer hydrogel in order to ensure that it will undergo safe and rapid degradation within the body. Rapid degradation within the wound site is vital to preventing the material from interfering with the body's natural healing process. Additionally, research will focus on enhancing the tissue adhesiveness of the polymer hydrogel so that the material is better able to seal the wound site.

Finally, research will be conducted in order to investigate the ability of the polymer hydrogel to systematically deliver a therapeutic in a controlled manner to the injured site. A material capable of inducing effective hemostasis while simultaneously delivering a therapeutic to the wound site would have incredible potential in the healthcare field.

Overall, future research will focus on developing a better understanding of the material properties which affect the body's blood clotting response. A better understanding of the interactions that occur between engineered materials and the body's physiologic blood clotting response is the key to the development of next-generation blood contacting materials.

## Bibliography

1. Vogler, E.A. & Siedlecki, C.A. Contact activation of blood-plasma coagulation. *Biomaterials* **30**, 1857-1869 (2009).
2. Adams, R.L.C. & Bird, R.J. Review article: Coagulation cascade and therapeutics update: Relevance to nephrology. Part 1: Overview of coagulation, thrombophilias and history of anticoagulants. *Nephrology* **14**, 462-470 (2009).
3. Town, U.o.C. Blood Clot. (ed. Clot, B.) (Cape Town, South Africa, 2007).
4. Krug, E.G., Sharma, G.K. & Lozano, R. The global burden of injuries. *American Journal of Public Health* **90**, 523-526 (2000).
5. Peden M., M.K., Sharma G. . The Injury Chart Book: A Graphical Overview of the Global Burden of Injuries. (ed. Organization, W.H.) (2002).
6. Falati, S., Edmead, C.E. & Poole, A.W. Glycoprotein Ib-V-IX, a receptor for von Willebrand factor, couples physically and functionally to the Fc receptor gamma-chain, Fyn, and Lyn to activate human platelets. *Blood* **94**, 1648-56 (1999).
7. Chiang, T.M., Seyer, J.M. & Kang, A.H. Collagen-Platelet Interaction - Separate Receptor-Sites for Type-I and Type-Iii Collagen. *Thrombosis Research* **71**, 443-456 (1993).
8. Monnet, E., Fauvel-Lafeve, F. & Legrand, Y. Identification of a new platelet receptor specific for type III collagen. *Thrombosis and Haemostasis*, 639-639 (1999).
9. Ruggeri, Z.M. Platelets in atherothrombosis. *Nature Medicine* **8**, 1227-1234 (2002).
10. Cines, D.B. et al. Endothelial cells in physiology and in the pathophysiology of vascular disorders. *Blood* **91**, 3527-61 (1998).
11. Patek, A.J. & Stetson, R.P. Hemophilia. I. the Abnormal Coagulation of the Blood and Its Relation to the Blood Platelets. *J Clin Invest* **15**, 531-42 (1936).
12. Owren, P.A. The 5th Coagulation Factor (Factor-V) and Its Clinical Significance. *Acta Haematologica* **1**, 285-285 (1948).
13. Owren, P.A. The 5th Coagulation Factor (Factor-V) - Preparation and Properties. *Biochemical Journal* **43**, 136-139 (1948).
14. Alexander, B. et al. Congenital Spca Deficiency - a Hitherto Unrecognized Coagulation Defect with Hemorrhage Rectified by Serum and Serum Fractions. *Journal of Clinical Investigation* **30**, 596-608 (1951).
15. Aggeler, P.M. et al. Plasma thromboplastin component (PTC) deficiency; a new disease resembling hemophilia. *Proc Soc Exp Biol Med* **79**, 692-4 (1952).
16. Biggs, R. et al. Christmas disease: a condition previously mistaken for haemophilia. *Br Med J* **2**, 1378-82 (1952).
17. Hougie, C., Barrow, E.M. & Graham, J.B. Stuart Clotting Defect .1. Segregation of an Hereditary Hemorrhagic State from the Heterogeneous Group Heretofore Called Stable Factor (Spca, Proconvertin, Factor-Vii) Deficiency. *Journal of Clinical Investigation* **36**, 485-496 (1957).

18. Graham, J.B., Barrow, E.M. & Hougie, C. Stuart Clotting Defect .2. Genetic Aspects of a New Hemorrhagic State. *Journal of Clinical Investigation* **36**, 497-503 (1957).
19. Rosenthal, R.L., Dreskin, O.H. & Rosenthal, N. New Hemophilia-Like Disease Caused by Deficiency of a 3rd Plasma Thromboplastin Factor. *Proceedings of the Society for Experimental Biology and Medicine* **82**, 171-174 (1953).
20. Ratnoff, O.D. & Colopy, J.E. Familial Hemorrhagic Trait Associated with a Deficiency of a Clot-Promoting Fraction of Plasma. *Journal of Clinical Investigation* **34**, 602-613 (1955).
21. Delacadena, R.A. & Colman, R.W. The Sequence HgIghgheqhgIghgh in the Light Chain of High-Molecular-Weight Kininogen Serves as a Primary Structural Feature for Zinc-Dependent Binding to an Anionic Surface. *Protein Science* **1**, 151-160 (1992).
22. Kunapuli, S.P., Delacadena, R.A. & Colman, R.W. Deletion Mutagenesis of High-Molecular-Weight Kininogen Light Chain - Identification of 2 Anionic Surface Binding Subdomains. *Journal of Biological Chemistry* **268**, 2486-2492 (1993).
23. Schmaier, A.H. et al. Determination of the Bifunctional Properties of High-Molecular-Weight Kininogen by Studies with Monoclonal-Antibodies Directed to Each of Its Chains. *Journal of Biological Chemistry* **262**, 1405-1411 (1987).
24. Yarovaya, G.A., Blokhina, T.B. & Neshkova, E.A. Contact system. New concepts on activation mechanisms and bioregulatory functions. *Biochemistry-Moscow* **67**, 13-24 (2002).
25. Vandieijen, G., Tans, G., Rosing, J. & Hemker, H.C. The Role of Phospholipid and Factor-Viii in the Activation of Bovine Factor-X. *Journal of Biological Chemistry* **256**, 3433-3442 (1981).
26. Saenko, E.L., Shima, M. & Sarafanov, A.G. Role of activation of the coagulation factor VIII in interaction with vWf, phospholipid, and functioning within the factor Xase complex. *Trends in Cardiovascular Medicine* **9**, 185-192 (1999).
27. Price, G.C., Thompson, S.A. & Kam, P.C.A. Tissue factor and tissue factor pathway inhibitor. *Anaesthesia* **59**, 483-492 (2004).
28. Hoffman, M., Monroe, D.M., Oliver, J.A. & Roberts, H.R. Factors Ixa and Xa Play Distinct Roles in Tissue Factor-Dependent Initiation of Coagulation. *Blood* **86**, 1794-1801 (1995).
29. Davie, E.W., Fujikawa, K. & Kisiel, W. The Coagulation Cascade - Initiation, Maintenance, and Regulation. *Biochemistry* **30**, 10363-10370 (1991).
30. Mackman, N., Tilley, R.E. & Key, N.S. Role of the extrinsic pathway of blood coagulation in hemostasis and thrombosis. *Arteriosclerosis Thrombosis and Vascular Biology* **27**, 1687-1693 (2007).
31. del Zoppo, G.J. et al. Tissue factor localization in non-human primate cerebral tissue. *Thromb Haemost* **68**, 642-7 (1992).
32. Eddleston, M. et al. Astrocytes are the primary source of tissue factor in the murine central nervous system. A role for astrocytes in cerebral hemostasis. *J Clin Invest* **92**, 349-58 (1993).

33. Fleck, R.A., Rao, L.V.M., Rapaport, S.I. & Varki, N. Localization of Human Tissue Factor Antigen by Immunostaining with Monospecific, Polyclonal Anti-Human Tissue Factor Antibody. *Thrombosis Research* **57**, 765-781 (1990).
34. Flossel, C., Luther, T., Muller, M., Albrecht, S. & Kasper, M. Immunohistochemical Detection of Tissue Factor (Tf) on Paraffin Sections of Routinely Fixed Human Tissue. *Histochemistry* **101**, 449-453 (1994).
35. Lockwood, C.J. et al. Progestational Regulation of Human Endometrial Stromal Cell Tissue Factor Expression during Decidualization. *Journal of Clinical Endocrinology and Metabolism* **76**, 231-236 (1993).
36. Komiyama, Y., Pedersen, A.H. & Kisiel, W. Proteolytic Activation of Human Factor-Ix and Factor-X by Recombinant Human Factor-Viia - Effects of Calcium, Phospholipids, and Tissue Factor. *Biochemistry* **29**, 9418-9425 (1990).
37. Drake, T.A., Morrissey, J.H. & Edgington, T.S. Selective Cellular Expression of Tissue Factor in Human-Tissues - Implications for Disorders of Hemostasis and Thrombosis. *American Journal of Pathology* **134**, 1087-1097 (1989).
38. Faulk, W.P., Labarrere, C.A. & Carson, S.D. Tissue Factor - Identification and Characterization of Cell-Types in Human Placentae. *Blood* **76**, 86-96 (1990).
39. Smith, S.A. & Morrissey, J.H. Rapid and efficient incorporation of tissue factor into liposomes. *Journal of Thrombosis and Haemostasis* **2**, 1155-1162 (2004).
40. Harlos, K. et al. Vitamin-K-Dependent Blood-Coagulation Proteins Form Hetero-Dimers. *Nature* **330**, 82-84 (1987).
41. Sunnerhagen, M., Drakenberg, T., Forsen, S. & Stenflo, J. Effect of Ca<sup>2+</sup> on the structure of vitamin K-dependent coagulation factors. *Haemostasis* **26**, 45-53 (1996).
42. Sabharwal, A.K. et al. High-Affinity Ca<sup>2+</sup>-Binding Site in the Serine-Protease Domain of Human Factor Viia and Its Role in Tissue Factor-Binding and Development of Catalytic Activity. *Journal of Biological Chemistry* **270**, 15523-15530 (1995).
43. Neuenschwander, P.F. & Morrissey, J.H. Roles of the Membrane-Interactive Regions of Factor-Viia and Tissue Factor - the Factor-Viia Gla-Domain Is Dispensable for Binding to Tissue Factor but Important for Activation of Factor-X (Vol 269, Pg 8009, 1994). *Journal of Biological Chemistry* **269**, 16983-16983 (1994).
44. Baugh, R.J., Broze, G.J. & Krishnaswamy, S. Regulation of extrinsic pathway factor Xa formation by tissue factor pathway inhibitor. *Journal of Biological Chemistry* **273**, 4378-4386 (1998).
45. Broze, G.J. Tissue Factor Pathway Inhibitor and the Revised Theory of Coagulation. *Annual Review of Medicine* **46**, 103-112 (1995).
46. Riewald, M. & Ruf, W. Science review: role of coagulation protease cascades in sepsis. *Crit Care* **7**, 123-9 (2003).
47. Prockop, D.J. What holds us together? Why do some of us fall apart? What can we do about it? *Matrix Biology* **16**, 519-528 (1998).
48. Palm, M.D. & Altman, J.S. Topical hemostatic agents: A review. *Dermatologic Surgery* **34**, 431-445 (2008).

49. Krishnan, L.K., Mohanty, M., Umashankar, P.R. & Lal, A.V. Comparative evaluation of absorbable hemostats: advantages of fibrin-based sheets. *Biomaterials* **25**, 5557-5563 (2004).
50. Larson, P.O. Topical Hemostatic Agents for Dermatologic Surgery. *Journal of Dermatologic Surgery and Oncology* **14**, 623-632 (1988).
51. Ryan, E.A., Mockros, L.F., Weisel, J.W. & Lorand, L. Structural origins of fibrin clot rheology. *Biophysical Journal* **77**, 2813-2826 (1999).
52. Ryan, E.A., Mockros, L.F., Stern, A.M. & Lorand, L. Influence of a natural and a synthetic inhibitor of factor XIIIa on fibrin clot rheology. *Biophysical Journal* **77**, 2827-2836 (1999).
53. Hong, Y.M. & Loughlin, K.R. The use of hemostatic agents and sealants in urology. *Journal of Urology* **176**, 2367-2374 (2006).
54. Shekarriz, B. & Stoller, M.L. The use of fibrin sealant in urology. *Journal of Urology* **167**, 1218-1225 (2002).
55. Msezane, L.P., Katz, M.H., Gofrit, O.N., Shalhav, A.L. & Zorn, K.C. Hemostatic agents and instruments in laparoscopic renal surgery. *Journal of Endourology* **22**, 403-408 (2008).
56. Hidas, G. et al. Sutureless nephron-sparing surgery: Use of albumin glutaraldehyde tissue adhesive (BioGlue). *Urology* **67**, 697-700 (2006).
57. Furst, W. & Banerjee, A. Release of glutaraldehyde from an albumin-glutaraldehyde tissue adhesive causes significant in vitro and in vivo toxicity. *Annals of Thoracic Surgery* **79**, 1522-1529 (2005).
58. Erasmi, A.W., Sievers, H.H. & Wohlschlagel, C. Inflammatory response after BioGlue application. *Annals of Thoracic Surgery* **73**, 1025-1025 (2002).
59. Gabay, M. Absorbable hemostatic agents. *American Journal of Health-System Pharmacy* **63**, 1244-1253 (2006).
60. Torchiana, D.F. Polyethylene glycol based synthetic sealants: Potential uses in cardiac surgery. *Journal of Cardiac Surgery* **18**, 504-506 (2003).
61. Eaglstein, W.H. & Sullivan, T. Cyanoacrylates for skin closure. *Dermatologic Clinics* **23**, 193-+ (2005).
62. Citrin, P., Doscher, W., Wise, L. & Margolis, I.B. Control of Needle Hole Bleeding with Ethyl-Cyanoacrylate Glue (Krazy Glue). *Journal of Vascular Surgery* **2**, 488-490 (1985).
63. Landry, J.R. & Kanat, I.O. Considerations in Topical Hemostasis. *Journal of the American Podiatric Medical Association* **75**, 581-585 (1985).
64. Rysava, J. et al. Surface interactions of oxidized cellulose with fibrin(ogen) and blood platelets. *Sensors and Actuators B-Chemical* **90**, 243-249 (2003).
65. Dineen, P. Antibacterial Activity of Oxidized Regenerated Cellulose. *Surgery Gynecology & Obstetrics* **142**, 481-486 (1976).
66. Sabino, L. et al. Evaluation of renal defect healing, hemostasis, and urinary fistula after Laparoscopic partial nephrectomy with oxidized cellulose. *Journal of Endourology* **21**, 551-556 (2007).
67. Scher, K.S. & Coil, J.A. Effects of Oxidized Cellulose and Microfibrillar Collagen on Infection. *Surgery* **91**, 301-304 (1982).

68. Alam, H.B., Burris, D., DaCorta, J.A. & Rhee, P. Hemorrhage control in the battlefield: Role of new hemostatic agents. *Military Medicine* **170**, 63-69 (2005).
69. Sun, H., Apkarianj, R.P., Dublin, S.N., Levy, J.H. & Tanaka, K.A. Scanning electron microscopical observations of two novel hemostatic polymers. *Journal of Thrombosis and Haemostasis* **3**, 1537-1539 (2005).
70. Kuwahara, R.T., Craig, S.R. & Amonette, R. More on Monsel's solution. *Dermatologic Surgery* **26**, 979-980 (2000).
71. Epstein, E. & Maibach, H.I. Monsel's Solution - History Chemistry + Efficacy. *Archives of Dermatology* **90**, 226-& (1964).
72. Ratnoff, O.D. & Rosenblum, J.M. The Role of Hageman Factor in the Initiation of Clotting by Glass. *Journal of Laboratory and Clinical Medicine* **50**, 941-942 (1957).
73. Revak, S.D., Cochrane, C.G. & Johnston, A.R. Structure of Hageman-Factor in Its Native and Activated Forms. *Federation Proceedings* **32**, 845-& (1973).
74. Smith, S.A. & Morrissey, J.H. Polyphosphate enhances fibrin clot structure. *Blood* **112**, 2810-2816 (2008).
75. Bjorn S, T.L. Activation of coagulation factor VII to VIIa. *Research Disclosure* **269**, 564-565 (1986).
76. Pedersen, A.H., Lundhansen, T., Bisgaardfrantzen, H., Olsen, F. & Petersen, L.C. Autoactivation of Human Recombinant Coagulation Factor-Vii. *Biochemistry* **28**, 9331-9336 (1989).
77. Fiore, M.M., Neuenschwander, P.F. & Morrissey, J.H. The Biochemical Basis for the Apparent Defect of Soluble Mutant Tissue Factor in Enhancing the Proteolytic Activities of Factor-Viia. *Journal of Biological Chemistry* **269**, 143-149 (1994).
78. Griffith, M.J. et al. Characterization of the Clotting Activities of Structurally Different Forms of Activated Factor-Ix - Enzymatic-Properties of Normal Human Factor-Ixa-Alpha, Factor-Ixa-Beta, and Activated Factor-Ix. *Journal of Clinical Investigation* **75**, 4-10 (1985).
79. Lundblad, R.L. & Roberts, H.R. The Acceleration by Polylysine of the Activation of Factor-X by Factor Ixa. *Thrombosis Research* **25**, 319-329 (1982).
80. Lundblad, R.L., Vogel, C.N., Butkowski, R.J. & Mann, K.G. Effect of Polylysine on Activation of Prothrombin. *Federation Proceedings* **35**, 757-757 (1976).
81. Miller, K.D., Copeland, W.H. & Mcgarrahan, J.F. Agents Providing Nonenzymic Prothrombin Activation. *Proceedings of the Society for Experimental Biology and Medicine* **108**, 117-& (1961).
82. Vogel, C.N., Butkowski, R.J., Mann, K.G. & Lundblad, R.L. Effect of Polylysine on Activation of Prothrombin - Polylysine Substitutes for Calcium-Ions and Factor-V in Factor-Xa Catalyzed Activation of Prothrombin. *Biochemistry* **15**, 3265-3269 (1976).
83. Roberts, H.R., Monroe, D.M. & White, G.C. The use of recombinant factor VIIa in the treatment of bleeding disorders. *Blood* **104**, 3858-64 (2004).

84. S Sobieszczyk, G.B., B Kubiacyk, T Opala. Efficacy of recombinant activated Factor VII (rFVIIa; NovoSeven) in obstetrical haemorrhagic shock. *Critical Care* **7**, 105 (2003).
85. Oliver, J.A., Monroe, D.M., Roberts, H.R. & Hoffman, M. Thrombin activates factor XI on activated platelets in the absence of factor XII. *Arteriosclerosis Thrombosis and Vascular Biology* **19**, 170-177 (1999).
86. Lyon, M.E., Drobot, D.W., Harding, S.R. & Lyon, A.W. Evaluation of the thrombin inhibitor D-phenylalanyl-L-prolyl-L-arginine chloromethylketone (PPACK) with the factor Xa inhibitor 1,5-dansyl-L-glutamyl-L-glycyl-L-arginine chloromethylketone (GGACK) as anticoagulants for critical care clinical chemistry specimens. *Clinica Chimica Acta* **280**, 91-99 (1999).
87. Motlagh, D., Yang, J., Lui, K.Y., Webb, A.R. & Ameer, G.A. Hernocompatibility evaluation of poly(glycerol-sebacate) in vitro for vascular tissue engineering. *Biomaterials* **27**, 4315-4324 (2006).
88. Bajaj, S.P., Rapaport, S.I. & Brown, S.F. Isolation and Characterization of Human Factor-Vii - Activation of Factor-Vii by Factor-X. *Journal of Biological Chemistry* **256**, 253-259 (1981).
89. Jozefowicz, M. & Jozefonvicz, J. Antithrombogenic Polymers. *Pure and Applied Chemistry* **56**, 1335-1344 (1984).
90. K.G., M. Prothrombin. *Methods of Enzymology* **45**, 123-156 (1976).
91. Tracy, P.B., Eide, L.L., Bowie, E.J.W. & Mann, K.G. Radioimmunoassay of Factor-V in Human-Plasma and Platelets. *Blood* **60**, 59-63 (1982).
92. Thompson, A.R. Structure, Function, and Molecular Defects of Factor-Ix. *Blood* **67**, 565-572 (1986).
93. Hedner, U., Henriksson, P. & Nilsson, I.M. Factor 13 in a Clinical Material. *Scandinavian Journal of Haematology* **14**, 114-119 (1975).
94. Hashimoto, N., Morita, T. & Iwanaga, S. A Method for Systematic Purification from Bovine Plasma of 6 Vitamin-K-Dependent Coagulation-Factors - Prothrombin, Factor-X, Factor-Ix, Protein-S, Protein-C, and Protein-Z. *Journal of Biochemistry* **97**, 1347-1355 (1985).
95. Narayanaswamy, M., Wright, K.C. & Kandarpa, K. Animal models for atherosclerosis, restenosis, and endovascular graft research. *Journal of Vascular and Interventional Radiology* **11**, 5-17 (2000).
96. Ni, R.F. et al. Testing percutaneous arterial closure devices: an animal model. *Cardiovasc Intervent Radiol* **32**, 313-6 (2009).

